Topology Optimization of Dielectric Substrates for Filters and Antennas Using SIMP

G. Kiziltas

ElectroScience Lab., ECE Dept.
The Ohio State University
Columbus, OH 43212, USA
gkiziltas@esl.eng.ohio-state.edu

N. Kikuchi

The University of Michigan
Ann Arbor, MI, 48109-2121, USA

J.L. Volakis

ElectroScience Lab., ECE Dept.
The Ohio State University
Columbus, OH 43212, USA

J. Halloran

The University of Michigan
Ann Arbor, MI, 48109-2121, USA

Summary

In this paper a novel design procedure based on the integration of full wave Finite Element Analysis (FEA) and a topology design method employing Sequential Linear Programming (SLP) is introduced. The employed design method is the Solid Isotropic Material with Penalization (SIMP) technique formulated as a general non-linear optimization problem. SLP is used to solve the optimization problem with the sensitivity analysis based on the adjoint variable method for complex variables. A key aspect of the proposed design method is the integration of optimization tools with a fast simulator based on the finite element-boundary integral (FE-BI) method. The capability of the design method is demonstrated by two design examples. First, we developed a metamaterial substrate with arbitrary material composition and subject to a pre-specified antenna bandwidth enhancement. The design is verified and its performance is evaluated via measurements and simulation. As a second example, the material distribution for a Thermo-Photovoltaic (TPV) filter subject to pre-specified bandwidth and compactness criteria is designed. Results show that the proposed design method is capable of designing full three-dimensional volumetric material textures and printed conductor topologies for filters and patch antennas with enhanced performance.

1 INTRODUCTION

Evidence in literature demonstrates that use of artificial composite materials provides for a greater potential in designing new electromagnetic/RF devices [1–3]. However, existing studies dealing with design optimization for RF applications focused to a large extent on size or shape design only [4–7]. So far, material and topology optimization has not been pursued primarily due to the challenges associated with the fabrication of inhomogeneous materials and the limited access to versatile and efficient analysis tools. There are very few examples in the literature on topology optimization of electrical devices and these have dealt with problem specific, restricted or semi-analytic tools for magneto-static applications [8,9]. Here, our goal is to develop a general design method that draws from a broader class of design solutions as compared to conventional design methods and is capable of achieving topology and material designs for "new" electromagnetic devices with much higher performance.

In this paper, a topology optimization method based on the Solid Isotropic Material with Penalization Method (SIMP) is extended to develop full three-dimensional material topology designs for electromagnetic devices. The design problem is formulated in a non-linear optimization framework and is integrated with a fast full wave Finite Element-Boundary Integral (FE-BI) simulator. Solution of the optimization problem is obtained via the Sequential Linear Programming (SLP) with a sensitivity analysis based on the adjoint variable method for complex variables. This sensitivity analysis is specifically derived for the antenna's input impedance and filter's transmission coefficient and integrated into the simulator.

The capability of the proposed design method is demonstrated by two design examples. One example refers to the dielectric material topology of a patch antenna subject to pre-specified bandwidth and miniaturization criteria. The optimized design is post-processed via adaptive image filtering and is transformed into a two-material composite for manufacturability. The final substrate is manufactured using Thermoplastic Green Machining as a composite of Low Temperature Co-firing Ceramic (LTCC) filled with stycast polymer. In the second example, the dielectric substrate topology is designed for a spectral filter with bandpass behavior. Results from both miniaturized antenna and spectral filter case studies demonstrate the capability of the proposed method of designing full three-dimensional volumetric material textures for EM applications with enhanced performance.

2 BACKGROUND

This section provides an overview of the main milestones in electromagnetic (EM) design optimization. In the second part of the section, we present some background on topology optimization in structural mechanics and how it applies to EM. At the end of the section, we give some examples of topology optimization studies with the understanding that topology optimization refers only to the optimum material distribution approach.

2.1 Overview of Design Synthesis (Optimal Design) in EM History

The topic of optimal design in electromagnetics has a long history [10]. In other fields of engineering, the history of optimal design is even longer, dating back to Lagrange [11] and will be reviewed shortly in Section 2.2 in the context of structural topology optimization. Optimization theory in structural mechanics has had a history of 45 years. However, modern optimization theory as pertains to electromagnetics came much later. Among the pioneering works is that of Marrocco and Pironneau [12] who developed an optimum design of a magnet using lagrangian finite elements for modeling. Considering more general inverse problems in EM, it is appropriate to quote the fundamental contribution by Hadamard [13] who classified the optimization problem into two classes: well-posed and ill-posed classes.

As is well known, the solution of inverse problems is done iteratively. Historically, these iterations were carried out by cut and try operations taking months for each iteration or test. As a result, the design process relied on experience and intuition and was impractical. Today, modern optimization theory offers a great variety of automated techniques [14] for solving inverse problems in EM. These can be generally categorized in deterministic and stochastic techniques. Deterministic techniques (e.g. Simplex, Rosenbrock, gradient, quasi-Newton, Newton-Raphson, Sequential Quadratic Programming, Lagrangian Multipliers) seek the minimum point based on the information given by the negative of the gradient (sensitivity) of the objective function. Challenges in their implementation are the requirement to evaluate the gradient of the objective function and issues relating to the algorithm convergence. In contrast, gradient based techniques are mathematically well-behaved and do not involve heuristics. Hence, they are regarded as more attractive for most practical real world applications.

An early paper by Nakata and Takahashi [15] must be quoted in connection with gradient-based optimization. This paper presented a new design method for a permanent magnet employing the finite element method. The method was later applied by Hoole *et al.* [16] for the identification of cracks, sources and materials in inaccessible locations. Many others employed the same technique and variations exist in the sensitivity evaluation or the employed analysis module. Other applications of gradient based optimization include array synthesis and shape or size design of antennas. In general, gradient type methods have become prominent for large-scale topology optimization methods with thousands of design variables. They have also been applied to solve diverse multidisciplinary topology optimization problems.

With regard to gradient-free (stochastic methods) optimizers, their utilization has been quite substantial over the 1990's. Popular techniques in this category are simulated annealing (SA) and genetic algorithms (GAs) [17]. Although GAs were known since 1975 [18], their applications to EM problems occurred mostly in the early 1990s [19-21]. Indeed, GA's seemed adequate for the solution of global EM optimization problems, where the objective functions are non-convex and very often stiff, non-differentiable and ill-conditioned. Simulated annealing is analogous to the thermodynamic behavior of an annealed solid system slowly cooled to reach its lowest energy rate. Simkin and Trowbridge [22] employed this method successfully in combination with a direct search method for the solution of a classical shimming problem. Gottvald *et al.* [23] later showed, in a clear way, how the evolution strategy, simulated annealing and Monte-Carlo iteration are nothing but special interpretations of processes in biology, thermodynamics and statistics, respectively.

In addition to GA and SA, there are numerous other global techniques. Among them, the application of expert system in optimal design was proposed by Xueying *et al.* [24]. Also, artificial intelligence techniques have demonstrated a beneficial effect, when applied to solution of inverse electromagnetic field problems. In this respect, neural networks have been proposed [25] to solve problems at least in a limited domain of application. Fuzzy programming also seems to be useful in the solution of inverse problems or when used to improve the convergence of mathematical programming [26]. Recently, hybrid methods including design of experiments [27] and response surface methodology [28] have been proposed to combine the advantages of multiple optimization techniques.

In short, when dealing with inverse problems in EM, an adequate choice of optimization techniques becomes one of the central questions in their solution. In this context, Preis *et al.* [29] applied different evolution strategies to the optimal design of electromagnetic devices and showed the reciprocal advantages and disadvantages for the simple example of a magnet pole shape design. Gottvald *et al.* [23] examined some gradient based and stochastic optimization methods for the n-parameter optimization of magnetic systems. The choice of the algorithm was also considered by Bellina *et al.* [30] who compared and discussed deterministic and stochastic approaches. There are numerous other comparison studies [31] with most recent thorough investigations by Li *et al.* [32] demonstrating a comprehensive study of optimization algorithms combined with the Finite Element -Boundary Integral method for microstrip array design.

Due to the overwhelming literature and diversity of applications, the reader is referred to some reviews for detailed references to key studies in each field. A review for synthesis in EM related applications was given in [33]. Inverse EM problems were also reviewed by Guarnieri *et al.* [34] and an overview of optimal design methods for magnetic circuits was given by Takahashi [35]. For more recent investigations, the reader is referred to the studies by Di Barba *et al.* and Borghi [36] and the book by Neiitanmaki [37].

Naturally, it is not possible to identify a general-purpose method capable of solving all types of inverse problems in EM. Regardless of the optimization technique, the majority of the optimization algorithms are integrated with problem-specific/semi-analytic tools for

EM applications aimed to either improve the current design or speed-up the design process. Their main focus is typically that of size, shape or topology/material design of problems which can be separated in 3 categories: 1) magnetostatics 2) electrostatics and 3) electro-magnetodynamics. Examples falling into each category are discussed next.

Design of magnets, rotors and salient poles has attracted remarkable interest among magnetostatic applications. The linear two-dimensional magnet design [38] and its nonlinear version were demonstrated [39] and extended to include a three-dimensional model of the pole shape [40,41]. The solution of inverse problems in nuclear magnetic resonance (NMR) presents another classical problem [42]. In addition to NMR, one field with numerous contributions is that of non-destructive testing. There the focus is on eddy current tomography to identify position and shape of flaws and cracks in metallic structures [43]. Similarly, the best shape of coils has been defined [30] with more or less complicated configurations. The design of magnetic circuits has also been extensively analyzed [15,39].

Electrostatics, offers a number of shape synthesis/design problems as well. The synthesis of a capacitor [44], the optimal shape design of shielding electrodes [42] and the optimal design of an electrode [46] are among such problems. The boundary-element method has proved to be particularly convenient for electrostatic problems in homogeneous domains. It has been used with the least-squares approach for the identification of the boundary conditions in an electrostatic problem [47], and with a search technique [48] for the optimal shape design of an electrode. Using the finite-element method and a min-max approach, Sikora [49] solved the problem of locating an electrode in such a way that the resulting electric field intensity is as small as possible. Finally, electrocardiography is another inverse problem requiring the computation of potential values near and around the heart [50].

Electromagnetic radiation and scattering problems belong to the class of electro-magneto-dynamics and are among the most difficult to solve. Among typical electromagnetic optimization problems are those of antenna design, reflector antenna shaping [51], antenna array synthesis [52] for minimum sidelobe levels, antenna beam shaping [21], wire antenna design [53] and microstrip antennas and arrays for broadband performance [4], miniaturization and maximum efficiency. A popular method to solve these problems is the on/off approach of metallic elements. Stochastic methods such as simulated annealing or neural network are used for the solution of these problems. Often, brute force numerical methods (using the simplex method) are also employed to perform size optimization in designing FSS layers [54]. For the majority of antenna design problems, the dielectric constant of the spacers was assumed or selected from a predetermined database. The design problem was then limited to finding the surface resistivities of pre-determined metallic shapes and layer thicknesses.

Besides antenna design, optimization tools have also been widely used to design radar, satellite, and mobile communication systems. Design examples were demonstrated for stringent specifications such as pass-band insertion loss, stop-band rejection, power handling, and physical size of typically narrow-band bandpass devices. The goal is to determine the arrangement of coupled resonant circuits (resonators) to achieve a specified frequency-selective transfer function [55].

Other popular design problems include those of optimum design for broadband microwave devices involving layered material and anti-reflective coatings for low radar cross section (RCS) absorbers [56], frequency selective surfaces (FSS), radar target recognition and backscattering problems as well as wireless network layout design [19]. The development of methods for target image reconstruction [57] and the determination of permittivity distributions have attracted interest as well [58].

Regardless of the application area, the majority of design problems is limited to size and shape optimization. Very few topology and material optimization studies exist. More specifically, the focus has so far been on: 1) Size optimization for devices with a-priori known

shape and topology, 2) Shape optimization for parameters describing the unknown geometrical profile of a device with fixed topology and material, 3) Restricted material/topology optimization, where material and geometry is constructed from a discrete set of available materials/topologies pre-specified in a database and 4) Ill-posed topology optimization efforts where the geometric representation of devices is determined via an image based on/off approach.

Topology optimization methods are more general than size and shape optimization. They allow for changes in the topological configuration of the device, that is they allow for changes in the geometry, physical dimensions, connectivity of boundaries and material implants. Consequently, the possibility of topology design holds much greater promise since it dramatically increases the available degrees of freedom. Examples of restricted topology optimization those of shape design for microstrip antenna patches and material blocks forming the substrate have been mostly done using GA's. Here, the topology is not treated as a material distribution problem but is rather selected from a set of predetermined database. Further, the GA's are not as practical in solving generalized 3D topology optimization problems since they have extremely large CPU requirements and may become impractical due to their on/off design approach. Impracticality is an inherent drawback with stochastic methods. This is also related to the ill-posed formulation in the context of mathematical topology optimization. In fact, within the four groups of pursued design techniques, none is suited for addressing the topology and/or material aspect in a practical way.

The principle of "relaxation" [59] in topology optimization algorithms of electromagnetic systems is the same as that for structural systems. Relaxation has overcome the aforementioned mathematical difficulty in dealing with generalized topology optimization. The concept of three dimensional topology optimization relies on a specific form of relaxation and opens avenues for novel designs by distributing the available material in a given design domain. Background on topology optimization in structural mechanics is addressed in the next section. This is followed with related EM applications.

2.2 Topology Optimization for Structures

Optimization dates back to the fundamental design studies of Galileo [60], Lagrange [11] and Maxwell [10]. Mathematical programming techniques were developed in the late 1940s and early 1950s; the Finite Element Method (FEM) formulation was introduced by Courant [61] and set up by Clough [62] and Zienkiewicz [63]. Today, both tools represent the backbone of modern numerical optimization. It was Schmit [64] and later Zienkiewicz *et al.* [65] who initiated the integration of FEM with nonlinear mathematical programming for optimal structural design. Since then, the last three decades witnessed intensive research in the field of modern structural optimization. Much research work was subsequently devoted to the solution of practical optimization problems in a variety of applications including aeronautical, civil, mechanical and nuclear engineering. An early survey on optimal structural design is given by Venkayya [66]. More recent exhaustive collections with an emphasis on the fundamental aspects of optimal design are provided in [67] and [68]. Weeber *et al.*'s collection [69] gives a short review of structural design optimization as a source for developments in electromagnetics.

Structural optimization is usually divided into three areas: size, shape and topology optimization. Topology optimization, is sometimes called layout optimization, and is by far more general than any other existing design technique. Fundamental to topology optimization is that the connectedness of optimal structure is not assumed a priori.

Structural topology optimization methods are found in the literature dating back to 1904 (see Michell for truss-like structures [70]). These principles were extended later to grillages (beam systems) by Rozvany [71] who later [72,73] formulated the principles of optimal layout theory. The birth of (practical) FE-based topology optimization for non-

truss structures was brought about by the pioneering research of Bendsoe and Kikuchi who introduced the Homogenization Based Topology Optimization (HBTO) method [74].

Bendsoe and Kikuchi applied HBTO to find the optimum layout of a linearly elastic structure to achieve global stiffness. Since then, the HBTO method has become a common approach for determining the structural layout [75,76]. Their success to make generalized shape optimization practically possible for real designs was based on the idea of "designing thru material distribution" and "relaxation" of earlier ill-posed topology optimization problems. In the context of topology optimization of the linear elastic continua, a naive mathematical modeling of the physical problem is known to result in an ill-posed optimization problem. Typically, the problem is posed in terms of distributing an isotropic material in a fixed domain so that every domain point is associated with either filled or unfilled material. It was thru the pioneering work of Bendsoe and Kikuchi, that a partly relaxed version of the compliance minimization problem was solved. Their approach was amounted to introducing a periodic microstructure with rectangular inclusions from which the effective stiffness was determined by a homogenization formula. In technical terms, the homogenization method computes the macroscopic material properties on the assumption that a structure is full of microvoids. The macromaterial properties are then used in a regular finite element program to compute the compliance, i.e. the objective function for minimum compliance/stiffness problems, a classical problem in structural topology optimization. In short, the HBTO method is based on the assumption of a composite material with a microstructure whose properties are homogenized by a rigorous mathematical procedure. Typically, an algorithm based on the optimality criteria is used to update the size and orientation of voids.

Several other penalization techniques have been suggested. One strategy is to add a penalization term to the objective function [77]. Also, a specific full relaxation was proposed by Allaire and Kohn [78] for a special case of compliance problems. A more popular method is the so-called Solid Isotropic Material with Penalization (SIMP)/density formulation [72,79,80]. SIMP has been accepted as an alternative, or an obvious substitute to HBTO, especially for problems where the microstructure is not of a major concern. In SIMP, the material density in every finite element of the structure is treated as the design variable and intermediate density variables are penalized during the optimization process. A review on the origin, theoretical background, history, range of validity and major advantages of SIMP is provided in [73].

Unlike the homogenization method, in SIMP individual elements are considered to be isotropic and thus only one design variable is required for each element to characterize the design problem. Consequently, it is a powerful design method especially for multiphysics multi-material/composite problems with unknown microstructure details. More details will be discussed when presenting this design procedure. A comparison of SIMP and HBTO [72,79] as well as other approaches can also be found [73,81]. A different approach was proposed by Sankaranarayanan *et al.* [82] and their method is referred to as the simultaneous analysis and design method. This method has been used to determine the topology of two dimensional truss problems.

The principles of optimal layout theory were generalized considerably in the eighties and nineties [81]. Up to now, the most popular problem in topology optimization of linear elastic continua is that of minimizing compliance/stiffness for linear elastic structures. This problem has inherent attractive features that can be taken advantage of [81]. The underlying design principles are also extended to non-linear constitutive models [83]. In addition to elastic structures, the problem of designing compliant mechanisms was introduced by Ananthasuresh *et al.* [84]. The compliance topology designs have become popular challenging problems. The main objective for a compliant mechanism is to perform useful work on the workpiece, an objective that has resulted in different mathematical formulations in the

literature [85].

Early efforts in structural topology optimization were focused on a conceptual design with emphasis on global structural responses, such as stiffness, displacement and frequency only. However, later studies showed that the same topology optimization concept could be also powerful in other engineering applications such as automotive design. The concept is therefore used for problems relating to optimal weld/adhesive patterns or reinforcement patches for improving structural performance, and designing lightening holes for weight reduction [80]. It is also extended and proven to be useful in providing insight information for selecting better manufacturing processes.

Besides the more classical static problems, topology optimization methods are also applied to dynamic/frequency dependent problems to design structures such as car bodies, and to find optimal designs for minimizing vibration and noise, maximizing safety and minimizing product costs. Unlike the standard static mean compliance problems, in optimizing dynamic structures several different problems need be considered. The eigenvalue problem to find the optimal reinforcement of a plate-like structure [75], the frequency response problem [86] for optimum layout and optimum reinforcement problem and the transient response problem are some of them.

In short, the field of structural topology optimization has expanded significantly, addressing many practical engineering problems including maximum stiffness, maximum eigenvalue, optimum compliant mechanisms or piezoelectric actuators and extreme material properties. Moreover, design optimization has been accepted in industry, (with several commercial software packages now incorporating optimizations [87]). Comprehensive reviews from mechanical, structural and computational aspects have been given in the monographs by Bendsoe [79] and Hassani and Hinton [88] (see also the review article by Rozvany *et al.* [73]). The mathematical aspects of the concept are provided in [88]. Till very recent years, the majority of topology optimization methods were employed to solve linear, 'single physics' problems with a single constraint, such as the maximum stiffness optimization problem with the only constraint that of structural weight. However, recent developments in theory, computational speed and large-scale optimization algorithms allow us to extend this powerful method to problems involving multi-physics problems with multiple constraints and large number of elements. Nevertheless, existing studies are still limited to the design of thermally loaded structures, thermally/electrothermally actuated micro-devices, material microstructures with extreme thermo-elastic, piezoelectric or mechanical/electrical properties [89], and magneto-static applications [90]. Topology optimization problems involving geometrical non-linearities present another challenge. The recent extension of topology optimization to designing magnetostatic devices is largely due to the emergence of design sensitivity analysis and the availability of fast and rigorous numerical analysis codes. These will be reviewed in the next section.

2.3 Topology Optimization in EM

Gitosusastro introduced the concept of sensitivity for finite element analysis and its use in the optimization process for magnetic problems in 1988 [91]. More specifically, the "adjoint variable approach" was introduced [92] based on the method of sensitivity analysis used earlier in circuit theory, derived using Tellegen's theorem for electronic circuits. Since then, design sensitivity analysis using the adjoint variable method has been applied almost routinely to the optimization of magnetic devices. Applications include linear [93], nonlinear magnetic systems [94] and also linear electrostatic systems [95].

Optimization problems relying on the sensitivity information using the adjoint variable method (AVM) have been restricted to designing the shape of specific features of an otherwise complete device design. Examples are the pole shape of an electromagnet [96], slot

shape in the rotor of an induction motor [97] or the shape of a defect in an aluminum block [93].

To better exploit topology optimization algorithms in structural mechanics, the concept of parameterization to represent magnetic devices and perform topology optimization via the Optimum Material Distribution (OMD) approach was introduced by Dyck and Lowther *et al.* [98,92]. Topology optimization followed the same exact approach as in structural mechanics and was thereby introduced to the EM community using SIMP [90]. In these pioneering studies, gradients were evaluated efficiently via the adjoint variable method. For instance, SIMP was applied to the design of a "jumping ring" (or equivalently jumping bearing), a typical simple magneto-static problem. The study was the first to demonstrate the possibility for a 2D multi-material design with the permeability and the source current as the design attributes. Although the application was restricted to simple magnetostatic problems, the concept of automated topology design was introduced to the EM community. In the same study, fabrication challenges and the need to use manual intuitive filtering for solidification of the design were also addressed. In his PhD work, H. B. Lee, applied the same procedure to obtain a matched load in a waveguide structure [99].

Most of the later work on this topic are similar contributions by Dyck and Lowther. They interpreted the resulting gray-scale material distribution of the design by relating it to composites of available materials [100]. More specifically, they proposed to relate intermediate materials at the early stages of the design cycle to composite materials, which might be constructed from a number of solid materials to speed up the process of general shape optimization. In another study, the application of threshold image processing techniques was introduced to determine boundary shapes of optimized magnetic permeable material [101]. The focus was on image processing techniques to solidify gray scale images resulting from topology design of an induction furnace. Common to a series of similar works was the design of a magnetostatic system and a simple solution of decoupled FE system equations. Another characteristic of the model that led to a simplified design process in similar studies was the presence of real valued matrix equations instead of system equations with usual complex variables. The same concept was applied for a few more similar magnetostatic applications [102].

Byun *et al.* [93] applied the SIMP method for the topology optimization in EM focusing on the design of a transformer coil. The problem was to solve an eddy current problem, (a simplified version of an EM application) requiring more complex analysis procedures. Later, the same authors extended the design method to a specific class of inverse problems, where the goal was to find the shape and location of the dielectric material embedded in different permittivity background [95]. With this study, topology optimization in EM was expanded from magneto-static or eddy current systems to 3D linear electrostatic problems. The applicability of the sensitivity method and the idea of OMD have recently been tested on inverse scattering problems using FDTD for 2D scattering problems [103] and a 2D dielectric lens [104]. The most recent SIMP example in the literature is the topology optimization of a non-linear magneto-static device taking saturation effects into account [94]. This was a numerical study demonstrating the effect of saturation by comparing linear and non-linear topology optimization [105].

Besides SIMP, the application of the HDM method for topology optimization of linear magnetic devices has also been studied. The design focus, similar to earlier SIMP based studies, was a typical magnetostatic application: To design the shape of an H magnet by using an energy formulation [9]. The method was applied to two dimensional small-scale design problems, demonstrating the applicability of HDM to magnetic problems.

It is noted that the theoretical homogenization of electromagnetic system equations was pursued before it was actually applied to magnet design problems. The homogenized equations were derived for a heterogeneous elastic conductor in a magnetic field and later for

Maxwell's equations by Bossavit [106]. It was clearly demonstrated that the homogenization process for EM application is a frequency dependent process with the homogenized equations being cross-coupled following similar characteristics as chiral materials.

3 DESIGN PROCEDURE

In any automated optimum design approach (AOD) the goal is to identify in some automatic process the device structure and material composition subject to some prescribed performance. In this section, one such design process for the topology optimization of electromagnetic devices will be presented.

There are several different modules involved in the proposed design. Each of these has a particular function as will be discussed within the framework of the algorithm.

3.1 Analysis Method: Fast Spectral Domain Algorithm (FSDA)

As is the case with all numerical design optimization loops, the design process must incorporate a flexible and fast analysis module. It is of crucial importance that this module be fast without compromising the generality of the geometry and material composition of the device. The proposed design optimization procedure is based on the integration of such an analysis module (based on the hybrid finite-element boundary-integral method) with an optimization tool. Application of hybrid methods to infinite periodic structures allows for full 3-D modeling flexibility and allows for designing arbitrary geometrical and material details. More specifically, by virtue of the finite element method, the simulator is suitable for complex structures such as those involving inhomogeneous dielectrics, resistive patches, conducting patches and blocks, feed probes, impedance loads, and so on. This makes the simulator an ideal candidate for integrating with an optimizer.

The simulator employs the finite element method to model a unit cell (Figure 1) representing the doubly periodic array, whereas the boundary integral (BI) provides for a rigorous mesh truncation at the top and bottom surfaces of the discretized unit cell.
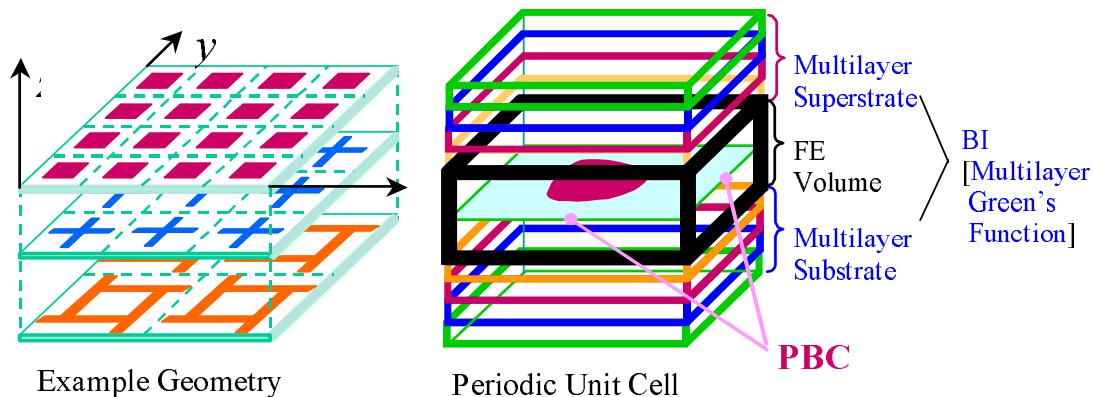

Figure 1. Doubly periodic array configuration and unit cell with BI termination on top and bottom surfaces and periodic boundary conditions at vertical sides in the FSDA

A key aspect of the periodic array model is the use of periodic boundary conditions (PBC's) to reduce the computational domain down to a single unit cell to significantly speed up analysis and reduce memory resources. More specifically, a fast integral equation algorithm is used for an efficient evaluation of the boundary integral termination referred to as the fast spectral domain algorithm (FSDA). The FSDA avoids explicit generation

of the usual fully populated method of moments matrix. Instead, at each iteration, the actual current distribution is summed up in the spectral domain, and the spectral Floquet mode series (for the BI) is then summed only once per testing function. Thus, for a fixed number of Floquet modes, the overall analysis method has O(N) memory demand and CPU complexity. Accurate results have already been obtained for scattering and radiation by cavities, slots, multilayer patch antennas and frequency selective surfaces, demonstrating the method's capability [55,107].

3.1.1 FE-BI formulation

The goal in any EM simulator is to solve the wave equation:

$$\vec{\nabla} \times \left(\frac{1}{\mu_r} \vec{\nabla} \times \vec{E} \right) - k_0^2 \varepsilon_r \vec{E} = -jk_0 Z_0 \vec{J^i} - \vec{\nabla} \times \left(\frac{1}{\mu_r} \vec{M^i} \right) \tag{1}$$

for the total electric field $\vec{E}$ throughout the computational volume V subject to a given set of boundary conditions on the surface enclosing the volume V. A representative computational volume is depicted in Figure 2 where

$\varepsilon_r, \mu_r :$ relative constitutive parameters of the material filling

$k_0 :$ free space wavenumber

$Z_0 :$ free space intrinsic impedance

$\vec{J^i}, \vec{M^i} :$ impressed electric/equivalent magnetic source

In its most general state, the computational domain is a three dimensional inhomogeneous body that may include embedded resistive card (R-card) surfaces, metallic elements, loads, feeds, and substrates with different permittivity and permeability. The source components $\vec{J^i}$ and $\vec{M^i}$ permit modeling of possible excitations (feeding sources) for antennas and vanish for scattering applications. For our specific analysis tool the computational domain is the unit cell for cascaded periodic layers with possible resistive and metallic elements. As discussed earlier, at the volume and surface boundaries (except the top surface S_{0t} and bottom surface S_{0b}) of the computational volume, periodic boundary conditions are applied. For more details on the implementation of the FE/BI method for cavity-backed antennas the reader is referred to [108] (see also Gong *et al.* [107] and [109]). Below we briefly present the general formulation to allow an understanding for its incorporation into an optimization loop.

The "heat" of any FEM-based code is the solution of the weak form of the vector wave equation (1) obtained using mathematical identities and the Green's divergence theorem. From [110], it follows that (1) can be cast in the form in conjunction with a weighting function $\vec{T}$ [110],

$$\int_V\!\!\int\!\!\int \left(\frac{1}{\mu_r} \left(\vec{\nabla} \times \vec{E} \right) \cdot \left(\vec{\nabla} \times \vec{T} \right) - k_0^2 \varepsilon_r \vec{E}\vec{T} \right) dV + jk_0 Z_0 \int_{S_0}\!\!\int \vec{T} \cdot [\vec{H} \times \hat{n}] dS +$$

$$+ \int_V\!\!\int\!\!\int \vec{T} \cdot \left(jk_0 Z_0 \vec{J^i} + \vec{\nabla} \times \left(\frac{1}{\mu_r} \vec{M^i} \right) \right) dV = 0 \tag{2}$$

In this, the aperture surface S_0 (all surfaces $= S_{0a} + S_{0b}$ in Figure 2) encloses the computational volume V, and $\hat{n}$ is the unit outward normal to S_0 where the magnetic field
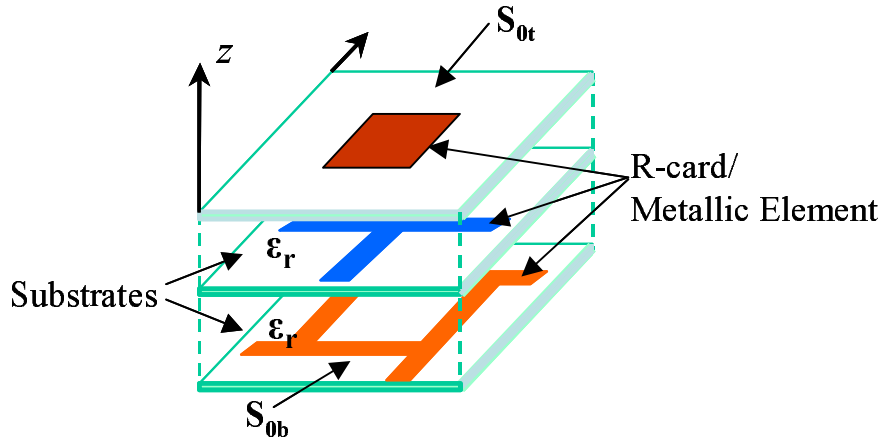
Figure 2. Representative computational domain (V) for finite element formulation

$\vec{H}$ exists. Basically, the first term in (2) is the volumetric contribution and the second term corresponds to the boundary integral contribution where the PBCs are explicitly enforced on the vertical walls. It is noted that it is necessary to enforce all boundary conditions within V and on S_0, implying the elimination of the magnetic field $\vec{H}$ by relating it to the electric field $\vec{E}$. On metallic surfaces we simply need to set the tangential components of E to zero. We remark that if the relation between $\vec{E}$ and $\vec{H}$ is a simple 1st or 2nd order boundary condition, the resulting matrix from equation (2) is sparse. However, if the relation between $\vec{E}$ and $\vec{H}$ is an integral equation, as required for exactness, then the resulting matrix is partly sparse and partly dense.

The exact details about the boundary conditions in the BI part via the spectral domain formulation were presented elsewhere and are not discussed here. The last term in (2) represents the excitation term due to antenna sources. It is remarked that the presence of resistive cards, coaxial cables, and lumped loads/conducting posts is easily accounted for by adding specific terms to (2).

To construct a system of equations for the solution of (2), the computational domain V is first subdivided into a number of finite elements (for example triangular prisms could be used and these naturally reduce to triangular elements on the top and bottom aperture surfaces). Each of these small elements occupies a volume V_e ($e = 1, \text{NFE}$) where NFE denotes the total number of elements in V. The field in each element is then approximated with a linear or a higher order expansion as follows:

$$\vec{E}^e = \sum_{j=1}^{m} E_j^e \vec{W}_j^e = \{\vec{W}^e\}\{E^e\} \tag{3}$$

where $\vec{W}_j^e$ denotes the edge based (vector) expansion basis functions. With this representation the expansion coefficients E_j^e are the unknowns at the jth edge of the eth element with m sides/edges.

Finally, Galerkin's method is applied and after the element matrices are assembled the conventional implementation of the hybrid FE/BI method for doubly periodic arrays leads to a linear algebraic system of the form:

$$[A]\{E\} + [Z]\{E\} = \{f\} \tag{4}$$

Here, $[A]$ is a complex valued square sparse matrix and is associated with the volumetric finite element portion of the hybrid method. Contributions of dielectric blocks or volumes and resistive cards or metallic edges in the unit cell are embedded in the $[A]$ matrix. The $[Z]$ matrix is associated with the edges on the top and bottom surfaces (S_{0t} and S_{0b}) of the discretized unit cell and is fully populated, i.e. it represents the BI part. The right hand side vector $\{f\}$ contains the excitations in the FE volume or BI apertures. The linear system is solved for the vector of unknown expansion coefficients $\{E\}$ representing the field unknowns.

3.2 Design via Topology Optimization

Simply stated, design via topology optimization implies the determination of the best arrangement given a limited volume of available (electromagnetic) material to the part of the domain so as to obtain an optimal (electromagnetic) performance. The optimization process systematically and iteratively eliminates and re-distributes material throughout the domain to obtain a concept structure. An attractive aspect of topology optimization is that it can be applied to the design of both materials and the geometry of devices.

When compared with more conventional size and shape optimization, where the topology of the device is assumed a priori and remains fixed, topology optimization offers much more degrees of freedom. Consequently, it is reasonable to expect that designs resulting from topology optimization have novel configurations with much higher performance. This optimization process has now reached a level of maturity and is consequently applied to many industrial problems for almost 20 years as discussed earlier in Section 2.

3.2.1 Density method

The design method employed here is based on the Density/Solid Isotropic Material with Penalization (SIMP) method. The SIMP method was proposed under the terms "direct approach" or "artificial density" approach by Bendsoe [79] over a decade ago; it was derived independently and used extensively by Rozvany *et al.* and others since 1990 [72,80]. The term "SIMP" was also introduced by the same author in 1992 [72]. After being out of favor with most other topology optimization researchers until recently, SIMP is nowadays accepted as a design technique of considerable advantages. For non-compliance problems and coupled field problems the optimal microstructures are not known. Therefore, either sub-optimal microstructures or other interpolation schemes must be used. Hence, SIMP is an ideal choice for our design problems. It is also very attractive to the engineering community because of its simplicity and efficiency [80,87].

SIMP synthesizes the device starting from any arbitrary topology. A key aspect of the design method is that any device, not known a priori, is represented by specifying the material properties at every point of the fixed design domain. For electromagnetic applications, these properties may be the permittivity and permeability of the dielectric material and conductivity/resistance of the metallic patches, etc. In practice, to specify material properties in the design region, the design space is discretized into material cells/finite elements. Actually, the most straightforward image-based geometry representation is the "0/1" integer choice, where the design domain is represented by either a void (no material) or a filled/solid material. Unfortunately, this class of optimization problems is ill-posed leading to non-convergent minimizing sequences of admissible designs [81].

It can be well posed via "relaxation" by incorporating microstructures into the extended design domain or allowing for material design with intermediate properties or continuous/graded properties. That is, the geometric representation of a device is similar to a gray-scale rendering of an image, in discrete form corresponding to a raster representation of the geometry. This is the essence of SIMP in which material grading is achieved during

design by introducing only a single density variable, ρ, and relating it to the actual material property of each finite element thru a continuous functional relationship. This material "law" models an artificial isotropic meta-material, mathematically manifested in the form of an empirical function, called the density function and represents the relationship between the material property (the relative permittivity (ε_r) and ρ. This scalar variable ρ can be physically interpreted as the density of the material whose properties are in proportion to ρ^n. A suitable density function, for the real permittivity (and possibly resistance of a metallic patch) would be:

$$\rho = \left[\frac{(\varepsilon_{\text{int}} - \varepsilon_{\text{air}})}{(\varepsilon_{\text{orig}} - \varepsilon_{\text{air}})} \right]^{1/n} \tag{5}$$

where n is a penalization factor; ε_{int} and $\varepsilon_{\text{orig}}$ are intermediate and original solid material permittivities, respectively.

The factor n is introduced to penalize the intermediate value of the density function. High values of the penalization factor decreases the permittivity of intermediate density elements, making such elements uneconomical if the volume is constrained and possibly active. That is, as n increases, intermediate values for the permittivity are less likely to occur, and hence the term penalization for intermediate material. However, this also increases the possibility of having different solutions that could be partially avoided by continuation methods [81,111]. The selection of n depends heavily on the problem type and is most of the time determined empirically.

The on/off nature of the problem formulation is avoided thru the material "law", i.e. the introduction of a normalized density with $\rho = 0$ corresponding to a void (air with ε_{air}), $\rho = 1$ to solid (original material $\varepsilon_{\text{orig}}$) and $0 < \rho < 1$ to a graded intermediate dielectric material (ε_{int}). This parameterization allows to formulate the problem in a general non-linear optimization framework. More specifically, the normalized density within each finite element is used as the design variable to formulate the topology/material optimization problem. The goal is to arrive at the optimum distribution of material (densities) such that the desired performance merit of a device is optimized subject to certain design constraints. This is achieved by assigning different density values from 0 to 1 in each design cell to represent the material variation from cell to cell. Unlike conventional optimization methods, such as the boundary variation or 0/1 representation of the design domain, the density method arrives at the optimum topology by distributing the material in the form of a gray scale image and updating it using standard gradient-based mathematical programming techniques. The density design method is then used in conjunction with standard optimization algorithms to achieve optimal material distribution designs for dielectric substrates such as those used in constructing band-pass frequency selective volumes or high bandwidth antennas as will be presented in Section 4.1. It is important to note that the permittivity of the material is assumed to be lossless, and hence the density function relates the real part of the actual complex permittivity to the real density variable. The construction of the optimization model will be discussed in the next section.

3.3 Optimization Model

The goal of the proposed design method is to establish a general formulation setting, which allows the determination of shape and topology/material distributions of EM devices within pre-specified performance requirements. The first step is to translate the design goals into a mathematical optimization model. This corresponds to the minimization of a cost function subject to design constraints. A standard formulation for optimization problems is to find the set of design variables x_i that will minimize/maximize the objective function

$$f(x_i) \tag{6}$$

subject to

$$h(x_i) = 0 \tag{7}$$

$$g(x_i) \leq 0 \tag{8}$$

and side constraints:

$$x_i^l \leq x_i \leq x_i^u \qquad i = 1, \ldots, N \tag{9}$$

where $f(x_i)$ is the objective function, $h(x_i)$ is the equality constraint and $g(x_i)$ is the inequality constraint. Also, x_i^l and x_i^u are the lower and upper bounds, respectively on the ith design variable of N total design variables. The objective and constraint functions can be multiple functions in a more general problem formulation setting.

The material distribution paradigm for the topology design problem is defined in a fixed design domain. In this domain, we seek the optimum distribution of material, with the term optimal being defined for the specific choice of the optimization model. An appropriate model for the proposed topology design procedure of electromagnetic material distribution/design problems employing the SIMP method would be to find the design variables ρ_i to minimize the cost function:

$$f(\rho_i(\varepsilon_i)) \tag{10}$$

subject to a volume constraint:

$$\sum_{i=1}^{N} \rho_i V_i \leq V^* \tag{11}$$

and side constraints:

$$0 \leq \rho_{\min} \leq \rho_i \leq \rho_{\max} \qquad i = 1, \ldots, N \tag{12}$$

with the following variable/parameter descriptions:

ρ_i :   normalized density variable of ith design cell/FE

ε_i :   permittivity of ith design cell/FE

V_i :   volume of ith design cell/FE

V^* :   upper limit for material volume of the design domain

N :   total number of design variables

$\rho_{\min}$:   lower bound on normalized density value

$\rho_{\max}$:   upper bound on normalized density value

The selection of the objective function and additional constraints may vary from problem to problem. Two specific design examples will be studied in Section 4 for which the details of each problem will be explained. However, the above formulation is versatile and allows for any post-processed performance metric function f (e.g. the bandwidth of a patch antenna or the transmission coefficient of a spectral filter). In its most general form, it is a function of the permittivity which is linked to design variables via the density function (5) and problem specific design parameters. Among possible design parameters are: geometrical, physical

and excitation details such as patch shape, dielectric thickness, and the presence of a feed/incoming wave. It is important to also note that the objective/constraint functions are usually frequency dependent quantities and require evaluations at each sampled frequency of the design spectrum.

The volume constraint is basically imposed to limit material usage. That is, a maximum volume V^* of the material is allowed within the design domain. The actual material volume is equal to the LHS function of the volume constraint, i.e. the sum of densities ρ_i and volume V_i of each design cell in the FE domain. Other reasons to include the volume constraint in the optimization model are as follows: First, for problems where the volume constraint is active, evidence in literature shows that optimization does actually result in a "black and white" design (if one chooses n sufficiently large). Without the volume constraint, islands of material that are disconnected from the actual device may appear. These superfluous islands may prevent the realization of the structure. Furthermore, without the volume constraint, the idea of the density function is lost and there is risk of ending up with structures with large gray regions. Second, for specific problems the volume constraint is associated with competing tradeoffs as is the case for the patch antenna design in achieving miniaturization.

The side constraints are needed to allow for material usage within prescribed limits of chosen (typically available) materials where $\rho_{\min}$ and $\rho_{\max}$ refer to the normalized lower and upper bound vector (unity), respectively.

The design formulation given in (10)–(12) is easily recognized as a general non-linear optimization problem with several thousands of design variables associated with the FE cells. This makes the use of gradient-based optimization techniques such as Sequential Linear Programming (SLP) a must for the solution of the optimization problem. The mathematical programming method for the solution is addressed next.

3.4 Mathematical Programming Method

Topology optimization problems with only one constraint can often be solved by more or less theoretically well-founded optimization algorithms. Examples are optimality criteria, evolutionary algorithms, hard-kill/soft-kill methods, etc. Many of these methods are based on intuition and make little or no use of sensitivity information that can be obtained computationally in an effective way. However, when considering more complicated objective functions and multiple constraints, none of these methods will be able to do a good job. Indeed, optimizations problems for EM systems in their most general form often require several constraints and many thousands of variables. Therefore, they fall within the "advanced" class of topology optimization problems and must be solved with theoretically well-founded mathematical programming methods making use of sensitivity analysis approximation concepts, and possibly, information from prior iterations. Example algorithms include the Sequential Linear Programming (SLP), CONLIN or the method of moving asymptotes (MMA). The iterative optimization scheme implemented here is the sequential linear programming (SLP) method employing the DSPLP computational package in the SLATEC library [112] for the numerical solution of the optimization problem.

The SLP method was successfully used in the optimization of truss structures [111]. It is also considered as a robust, efficient, and easy to use optimization algorithm in a review by Schittkowski and has been used for large-scale topology optimization problems in [113].

SLP consists of the sequential solution of an approximate linear sub-problem. More specifically, in each optimization iteration, the objective function and constraints are replaced by linear approximations obtained from the Taylor series expansion about the current design points (design vector), i.e. $x_i = \vec{x} = \{\vec{\rho}\}$. The linear programming sub-problem is then posed to find optimal design change vector $\Delta \vec{x}$ from the current design point at each iteration k. The SLP can be mathematically stated as follows.

Minimize the linearized objective function:

$$f(\vec{x}^{\langle k \rangle}) + \sum_{i=1}^{N} (\Delta x_i) \left(\frac{\partial f}{\partial x_i} \right) \Bigg|_{x^{\langle k \rangle}} \tag{13}$$

for N design variables, i.e. the optimal design change vector:

$$\Delta \vec{x} = \vec{x}^{\langle k+1 \rangle} - \vec{x}^{\langle k \rangle} \tag{14}$$

subject to the linearized volume constraint:

$$V_{\min}^{(m)} - V^{(m)}(x^{\langle k \rangle}) \leq \sum_{i=1}^{N} \Delta x_i \left(\frac{\partial V^{(m)}}{\partial x_i} \right) \Bigg|_{x^{\langle k \rangle}} \leq V_{\max}^{(m)} - V^{(m)}(x^{\langle k \rangle}) \tag{15}$$

and subject to the jth linearized constraint g:

$$g_j^{\min} - g_j(x^{\langle k \rangle}) \leq \sum_{i=1}^{N} \Delta x_i \left(\frac{\partial g}{\partial x_i} \right) \Bigg|_{x^{\langle k \rangle}} \tag{16}$$

and

$$(\Delta x_i)_{\min} \leq (\Delta x_i) \leq (\Delta x_i)_{\max} \tag{17}$$

Additional constraints can be included as well. In any case, these last set of constraints stand for move limits, with $(\Delta x_i)_{\min}$ and $(\Delta x_i)_{\max}$ being the lower and upper bounds on the allowable change in the design variables. The applied move-limit strategy is important for stable convergence of the algorithm. Here we use a move limit strategy originally proposed by Thomas et al. [114]. This technique is known to avoid locking of move limits in the case of exceedingly small design variables. The basic principle is to set the value for the max/min change in the ith design variable Δx_i such that:

$$\Delta x_i = \max(C x_i, (\Delta x_i)_{\min}) \tag{18}$$

where C is a constant defining the max change as a percent of the variable, and $(\Delta x_i)_{\min}$ is the minimum move limit in (17). For our design problems, C is set to 0.1 and $(\Delta x_i)_{\min}$ is set to approximately 1% of the upper bound of the design variable, i.e. 0.001. When the objective function reaches the proximity of the optimal value, the constant move ratio is decreased to half of the original value.

Upon optimization of a sub-problem, a new set of design variables, i.e. $\vec{x}^{\langle k+1 \rangle} = \vec{x}^{\langle k \rangle} + \Delta \vec{x}$ is obtained and updated in each design cell/finite element. As a result, the design domain has a new topology with an effective dielectric permittivity yielding a performance closer to the specified targets. The iterations proceed until convergence in the objective function is achieved. Substantial computational time can, of course, be saved if the starting guess is close to the optimal topology. More details about specific values and functions of optimization models will be provided for corresponding design problems.

To solve the linearized sub-problem above (13–17), the sensitivities of electromagnetic performance metrics (with respect to changes in the design variables x_i) are needed. This is discussed next.

3.5 Overview of Sensitivity Analysis

As mentioned earlier, the iterative process towards the minimum of the objective function may be accomplished by either derivative-free approaches or by gradient-based approaches. Using a gradient-based approach, the sensitivity analysis (which refers to the evaluation of derivatives of the objective function with respect to design variables) is the most critical and tedious step in the numerical solution procedure. In the early stages of its development, the sensitivity analysis was performed by finite difference techniques. That is, every design variable x_i was varied infinitesimally at a time and $f(x_i)$ was recomputed through a field computation for the new set of parameters. The ratio of the changes in $f(x_i)$ and x_i corresponded to the gradient with respect to each parameter x_i. However, this process was costly since for a problem with N design variables, the electromagnetic fields need to be computed $N+1$ times at each iteration of the design cycle. An alternative was whereby the gradients were computed without a second field solution [16, 91]. This was accomplished using the differentiability of the finite element and boundary element matrices [44].

There are two basic approaches for deriving the sensitivity. The first approach amounts to differentiating the discretized equations [49,91]. The second method, known as the continuous method, operates on the variational governing equations before they are discretized for the finite-element method [97] or the boundary-element method [96]. For the evaluation of the shape design sensitivity another method based on the material-derivative concept of continuum mechanics has also been used.

A standard and efficient way of calculating the design sensitivity expressions for the nonlinear electromagnetic radiation and scattering problems is the adjoint variable method. In the EM community, Director and Rohrer [115] are usually cited for the adjoint circuit approach for the sensitivity evaluation based on Tellegen's theorem. The essential feature of the method is the simple relation between the original circuit and the auxiliary or "adjoint" circuit (e.g., transpose of the nodal admittance matrix). As a result, the computational effort to evaluate the first-order derivatives of any response with respect to all design parameters is reduced to the analysis of a circuit pair.

The microwave literature abounds with techniques and applications using generalized scattering parameters, voltage-current variables, and branched cascaded topologies (for waveguide multiplexers). Sensitivities have been extracted for nonlinear magnetic analyses, and approximations based on the feasible adjoint sensitivity technique have been introduced. In the 1990s, the application of the adjoint network method to full-wave modeling of microwave structures was also employed. The adjoint variable method facilitates the analysis of non-linear circuits and their optimization using gradient based optimizers.

We will adopt herewith this adjoint variable technique for the derivation of the sensitivity to be used in connection with complex valued electromagnetic response functions (the transmission coefficient and return loss). The process will be discussed briefly in the next section and is based on the discrete form of the adjoint variable method. That is, the finite element formulation is used to perform analytical differentiation because of its computational efficiency and high accuracy. Specific details in deriving the transmission coefficient and return loss sensitivities are given in [116].

3.5.1 Derivation of sensitivity terms

Computation of the objective function derivatives with respect to the design variables is referred to as the "sensitivity analysis" and is of great importance to any gradient-based optimization technique. In a general EM design problem, the objective function (return loss, $|s_{11}|$ magnitude or transmission coefficient, $|\tau|$ etc.) is a post processed real-valued quantity based on the results of the FEM analysis module. More specifically, the performance metric depends on the unknowns solved via the FE simulator and can be expressed mathematically

by the function:

$$f = |F| = f(E_j(\varepsilon_i(\rho_i)), \varepsilon_i(\rho_i)) \qquad i = 1, \ldots, N \tag{19}$$

where $|F|$ refers to the post processed real-valued quantity (e.g. $|s_{11}|$, $|\tau|$) and ε_i represent the relative dielectric permittivities for the ith discrete element, i.e. the material property of the device to be optimized. The permittivity of a material is a complex valued quantity but if the material is assumed lossless in the design process, then ε_i denotes a real quantity with no loss (imaginary part). As defined earlier, ρ_i represents the set of element densities and E_j is the set of the complex valued unknown field coefficients solved by the hybrid FE-BI method using (4).

It is important to note that for most EM design problems, the objective function f is a real valued function of both complex (E_j) and real variables (ρ_i, ε_i, etc.). It must also be computed for the whole frequency spectrum of interest. Since in numerical analysis the spectrum is defined at a set of frequency points, the sensitivity analysis must be carried out for each frequency point and consists of the following steps:

1. The derivatives of $|F|$ (a real-valued function in 19) with respect to the output variable F (complex) is evaluated via an approximation [92], which resembles the classical chain rule of differentiation. Using this approximation, the derivative of the function of interest, f, with respect to the ith permittivity, ε_i is given by:

$$\frac{d|F|}{d\varepsilon_i} \cong \left\{ \frac{\partial|F|}{\partial\text{Re}(F)}\text{Re}\left[\frac{\partial F}{\partial\varepsilon_i}\right] + \frac{\partial|F|}{\partial\text{Im}(F)}\text{Im}\left[\frac{\partial F}{\partial\varepsilon_i}\right] \right\} \tag{20}$$

2. The chain rule differentiation is subsequently applied to evaluate the desired sensitivity term with respect to the actual design variables, ρ_i. This gives,

$$\frac{d|F|}{d\rho_i} = \left\{ \frac{\partial|F|}{\partial\text{Re}(F)}\text{Re}\left[\frac{\partial F}{\partial\varepsilon_i}\right] + \frac{\partial|F|}{\partial\text{Im}(F)}\text{Im}\left[\frac{\partial F}{\partial\varepsilon_i}\right] \right\} \left\{ \frac{\partial\varepsilon_i}{\partial\rho_i} \right\} \tag{21}$$

3. The last term $\frac{\partial\varepsilon_i}{\partial\rho_i}$ in (21) is easily evaluated by differentiating the density function (5). To evaluate the derivative term $\frac{\partial F}{\partial\varepsilon_i}$, chain rule differentiation is again applied to obtain

$$\frac{\partial F}{\partial\varepsilon_i} = \frac{\partial F}{\partial E_j}\frac{\partial E_j}{\partial\varepsilon_i} \tag{22}$$

Next, the derivative of the field coefficients E_j is obtained using the stiffness matrix $[A]$ of the FE-BI system. We have

$$\frac{\partial[A]}{\partial\varepsilon_i}\{E\} + [A]\frac{\partial\{E\}}{\partial\varepsilon_i} = \frac{\partial\{f\}}{\partial\varepsilon_i} \tag{23}$$

Rearranging, gives:

$$\frac{\partial\{E\}}{\partial\varepsilon_i} = [A]^{-1}\left(\frac{\partial\{f\}}{\partial\varepsilon_i} - \frac{\partial[A]}{\partial\varepsilon_i}\{E\}\right) \tag{24}$$

4. Substituting (24) into (22) results in

$$\frac{\partial F}{\partial \varepsilon_i} = \frac{\partial F}{\partial \{E\}} [A]^{-1} \left(\frac{\partial \{f\}}{\partial \varepsilon_i} - \frac{\partial [A]}{\partial \varepsilon_i} \{E\} \right) \tag{25}$$

5. Denoting term $\frac{\partial F}{\partial \{E\}}[A]^{-1}$ as λ:

$$\{\lambda\} = \frac{\partial F}{\partial \{E\}} [A]^{-1} \tag{26}$$

allows us to generate the expression

$$[A]\{\lambda\}^{\mathrm{T}} = \left\{ \frac{\partial F}{\partial \{E\}} \right\}^{\mathrm{T}} \tag{27}$$

Equation (27) is now recognized as the system matrix for the solution of the adjoint variable $\{\lambda\}^{\mathrm{T}}$ and is rearranged in the following form:

$$\{\lambda\}^{\mathrm{T}} = [A]^{-1} \left\{ \frac{\partial F}{\partial \{E\}} \right\}^{\mathrm{T}} \tag{28}$$

The above expression corresponds to the transpose solution (adjoint variable) of the original FE-BI matrix system (4). More specifically, the coefficient matrix $[A]$ is the same but the RHS vector $\{f\}$ is replaced with the derivative expression $\left\{ \frac{\partial F}{\partial \{E\}} \right\}^{\mathrm{T}}$. In fact, due to the symmetric nature of $[A]$, the transpose of (28) is equal to:

$$\{\lambda\} = \left\{ \frac{\partial F}{\partial \{E\}} \right\} ([A]^{-1})^{\mathrm{T}} = \left\{ \frac{\partial F}{\partial \{E\}} \right\} [A]^{-1} \tag{29}$$

and thus an iterative solution of (27) is equal to the desired first term λ in (25).

6. To evaluate the term in the parantheses of (25), the derivative $\frac{\partial \{f\}}{\partial \varepsilon}$ and $\frac{\partial [A]}{\partial \varepsilon}$ are computed on the local element level only and this allows for substantial CPU savings (only the local element matrices within the FE analysis formulation need to be differentiated). Finally, the resulting $\frac{\partial [A]}{\partial \varepsilon}$ expression is multiplied with edge expansion coefficients $\{E\}$ to complete the evaluation for the derivative expression in (25).

7. At each iteration step, the actual sensitivity term $\frac{d|F|}{d\rho}$ in (21) needed for each design variable at the sampled frequency is obtained by inserting the real and imaginary parts of the expression evaluated in step 7 into (25).

3.6 Computational Algorithm

The proposed design procedure as given above involves several algorithms and related interface modules. The resulting design algorithm was implemented in a custom-made code written in FORTRAN90. A simple in-data file allows for simplified entering of the design problem, material data and constraints. A separate user-interface is then used to pass the data between the FE-BI solver and the optimization routine. The final outputs are the input impedance and/or return loss. However, the actual distribution of the ε_i values are of
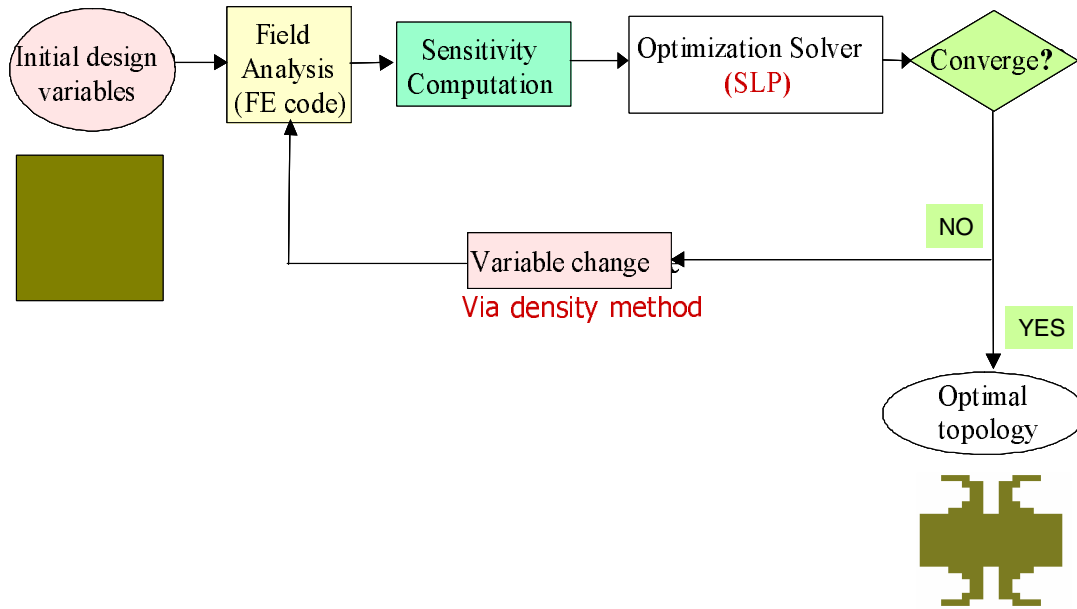
Figure 3. Design optimization flowchart

most interest and these can be displayed in 3D using SDRC IDEAS or other post-processing packages.

The algorithm for the proposed design cycle is shown in Figure 3. The design cycle starts with the initialization of design variables (set to represent a uniform dielectric). The design parameters are also specified at this step and do not change during the design cycle. These include patch geometry and material characterization such as the (1) dielectric block dimensions, (2) the feed location and its amplitude and, (3) the frequency range of operation. Optimization related parameters correspond to (1) penalization factor, (2) constraints on available material, (3) move limits, etc. The next step is to discretize the design domain into finite elements and to distribute the available dielectric material throughout the domain. Consequently, the design proceeds with the following iteration steps till convergence is achieved:

1. Simulation of device performance using the FE-BI solver and initial data.

2. Solution of adjoint system equations (27) and computation of related sensitivity terms.

3. Solution of the optimum material distribution problem using an SLP algorithm.

4. Update of design variables (densities/permittivities of design cells) via the SIMP interpolation scheme and move-limit strategy.

Convergence is achieved when the changes in the objective function value drop below a certain value (typically 10^{-3}). One can get a general idea of the final topology in less than 50 iterations depending on the complexity of the design problem. As can be expected, the whole design process may take from a few minutes to several hours on a modern workstation (1 GHz to 2.4 GHz processors). Computational time can be minimized if the starting guess is close to the optimal topology. Thus, as a rule, we begin with a rough/coarse mesh design, which must nevertheless still satisfy FE modeling accuracy requirement. The design domain may be subsequently divided into finer elements to form a refined model for the later optimization steps.
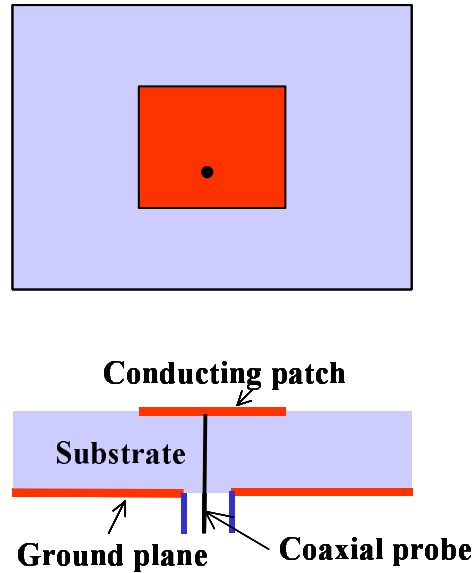
Figure 4. Probe fed rectangular patch on a grounded substrate

4 DESIGN EXAMPLES

4.1 Miniaturized Printed Antenna with Bandwidth Enhancements

Microstrip patch radiators (schematically shown in Figure 4) are attractive, low-weight, low-profile antennas but suffer from low bandwidth [117]. Moreover, their bandwidths are further reduced as the substrate dielectric constant is increased for miniaturization. The need for design, preferably design optimization (routines) is pertinent to the competing physics of these metrics and has been in focus for the past two decades [118,119]. However, most conventional methods to overcome these problems dealt with pure geometry/metallization design [4,120] and with predefined topologies. In this section, we demonstrate the capability of the proposed topology design method to develop a small patch antenna subject to pre-specified bandwidth criteria. The goal is to improve the bandwidth performance of a chosen simple patch antenna by introducing a 3D high-contrast dielectric material composition via SIMP.

An initial homogenous substrate with $\varepsilon = 42$ is chosen to operate in the frequency range of interest (1–2 GHz sampled over 21 frequency points). The details of the initial design are displayed in Figure 5. An appropriate objective function for the described topology optimization problem would be to find the design variables ρ that minimizes the cost function:

$$f(\rho) = \min[\max(|s_{11}|_j)] \qquad j = 1, \ldots, N_{\text{freq}} \qquad (30)$$

Minimization of the highest return loss (s_{11}) among sampled frequency points N_{freq} is known to maximize the return loss bandwidth [4]. A volume constraint was set to 70% to limit the use of materials and to avoid trivial bandwidth improvement via lowering the dielectric constant. With each design cell being updated via the SIMP method and the SLP routine as discussed above, a graded volumetric design is obtained in 20 iterations. The computation time for the entire design process (with 4000 finite elements and 21 frequency points per iteration) was 17 hours on a Pentium 3 Processor. The converged material distribution is
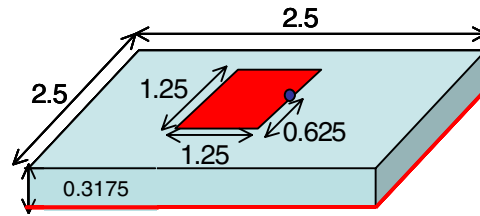
Figure 5. Initial patch antenna on homogeneous substrate (dimensions are in cm)
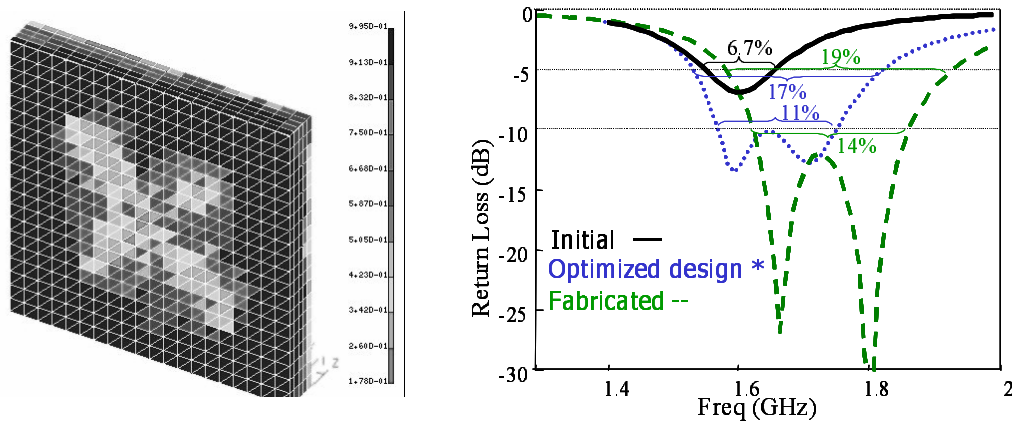

Figure 6. Optimized graded dielectric substrate (left) and return loss behaviour for initial, optimized and fabricated substrates (right)

displayed in Figure 6 as a 3D color-coded block with each color pixel corresponding to a certain permittivity value (density in scale bar). The corresponding return loss behaviors of the optimized and initial dielectric substrates are compared in Figure 6. Given the poor bandwidth at the starting point of the design, the attained bandwidth performance (with material design only) is truly remarkable.

To fabricate the design, certain post processing/image processing is necessary to transform the 3D gray-scale design into a solid two-material composite substrate. Due to its simplicity, image processing with a simple filtering strategy based on a cut-off value of 0.64 (for the densities) was adapted to solidify the design. The 3D composite substrate (Figure 7) is then fabricated using Thermoplastic Green Machining [121]. More specifically, first a thermoplastic compound is prepared by mixing commercially available Low-Temperature Cofirable Ceramic (LTCC- ULF 101) [121] powder with melted binder systems. Once compounded, it is warm-pressed and the dielectric block in its "green body" state is obtained. The material is machinable at this stage and has slightly larger dimensions than the expected design. After machining the substrate via computer-controlled drilling (Modela; Roland DG Corp., Japan), the substrate is sintered. To attain a smooth surface, the intricate holes are filled with a polymer stycast and a dielectric constant of 3 as depicted by the transparent material in Figure 7. The return loss behavior of the final fabricated substrate (dashed line) is compared to the initial substrate (solid line) and the optimized volumetric gray-scale design (dotted line) in Figure 6. As expected (due to filtering, man-
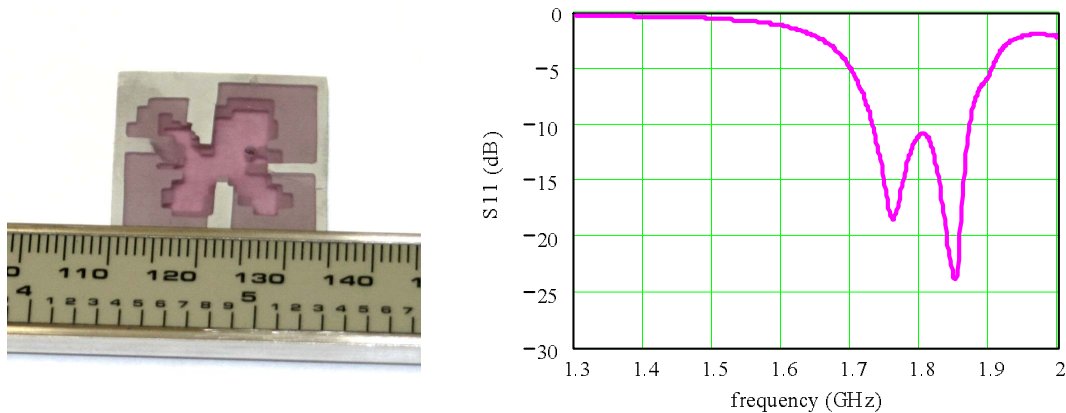
Figure 7. Fabricated two material composite substrate (left) (LTCC with $\varepsilon = 100$ filled with stycast polymer of $\varepsilon = 3$) and measured return loss behaviour with a probe fed patch antenna (Figure 5)

ufacturing alterations and stycast filling) the attained bandwidth for the fabricated design is different than its gray scale version obtained via topology optimization. In any case, the final attained bandwidth still exceeds design expectations by providing a threefold improved bandwidth performance with respect to the initial design. This demonstrates the power of integrating robust optimization techniques with simple filtering for manufacturable substrates for improved performance.

To validate the performance of the fabricated composite substrate, a square 1.25×1.25 cm conductor patch was painted on top of the final substrate using ECCOCOAT® C-110-5 silver. A coaxial probe feed was used to excite the patch as shown in Figure 5. The return loss measurements are depicted in Figure 7. It is noted that the bandwidth and the nulls of the fabricated composite substrate agree very well with the simulations except for a frequency shift of about 100 MHz. This small shift is attributed to the inherent feed and patch location imperfections as well as the unavoidable manufacturing flaws.

4.2 Frequency Selective Structure with Inhomogeneous Substrates for a Thermo-Photovoltaic Filter

Frequency Selective Structures (FSS) find widespread applications as filters in microwaves and optics [122]. They comprise periodically arranged metallic patch elements or apertures within multiple layers of cascaded dielectrics and are primarily used to enhance the frequency selectivity of spatial filters [123]. In addition to the more traditional applications, emerging applications are low band-gap materials for spectral control filters [124]. An application relates to Thermo-Photovoltaic (TPV) cell panels [125] used in the production of small lightweight portable generators. In this case, need exists to protect the TPV panels from broadband radiation by employing high efficiency spectral control filters. However, these filters often lack compactness, good band-pass behavior or desired efficiency. Here, we present the design of such a TPV filter with band-pass characteristics in the form of a FSS and cascaded inhomogeneous dielectric substrates. The goal is to allow for more design flexibility adopting the outlined design method and using dielectric periodic structures to deliver a sharper filter response. The desirable passband is 1-2.4 μm with a sharp transition in power transmission at the band-gap wavelength of 2.4 μm. The key requirement is that the filter transmits more than 90% up to 2.4 μm and less than 10% beyond that range.
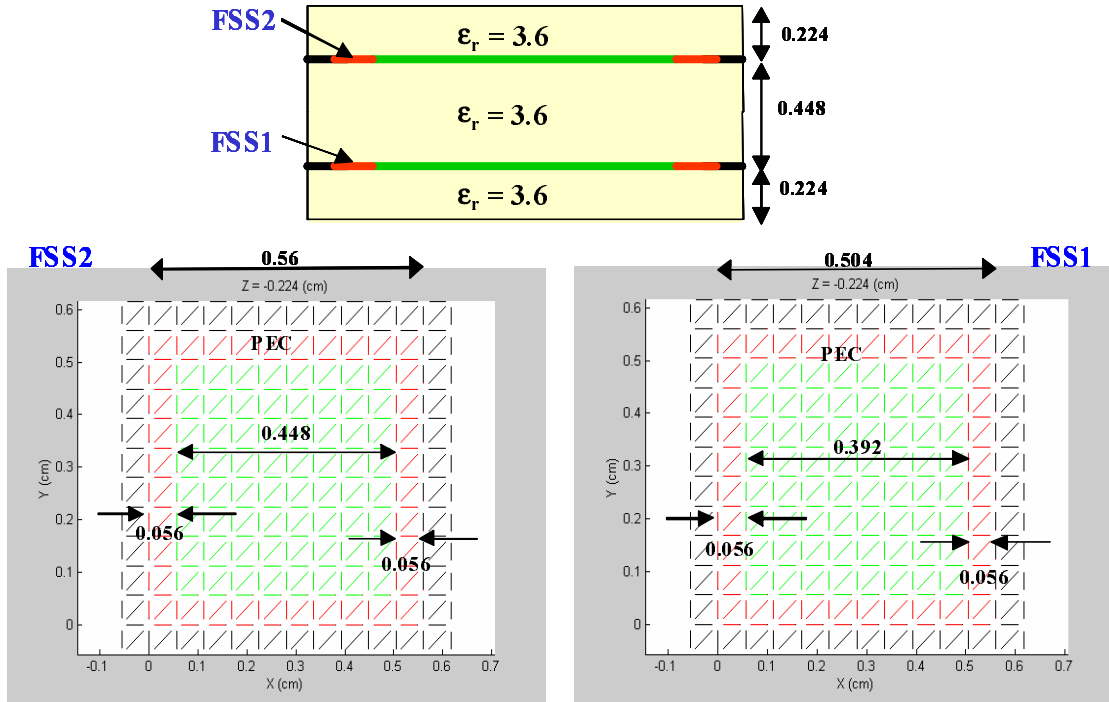
Figure 8. Illustration of the preliminary spectral filter design with double layer FSS sandwiched between $\varepsilon_r = 1.1$ substrates. Dimensions are in μm

Following basic design guidelines [126], primarily based on the FSS resonance behavior and the well-known quarter-wavelength transformer ($\lambda/4$) characteristics, we obtain the preliminary design configuration shown in Figure 8. This is a double layer non-commensurate FSS structure with wire loop shaped conductors (red crossing). However, the attained response using surface optimization required further refinement to improve the response by modifying the material/volume distribution.

Based on the design specifications and the proposed design procedure, a general nonlinear optimization problem with the following objective function was formulated:

Minimize

$$\sum_{\lambda_i=1}^{2.4} (|\tau_{\lambda_i} - 1|)^2 + \sum_{\lambda_i=2.4}^{4.6} (|\tau_{\lambda_i} - 0.1|)^2 \tag{31}$$

Here, τ_{λ_i} is the power transmission coefficient at wavelength λ_i. A minimum of the objective function corresponds to a performance with a high transmission ($\tau \sim 1.0$) for wavelengths 1-2.4 μm and a vanishing one ($\tau \sim 0.1$) for wavelengths out of that range (2.4-10 μm). Therefore, evenly spaced frequency points are chosen to ensure accurate capturing of the transmission response especially at the high frequency spectrum. To avoid high CPU costs for the simulation, only up to 4.6 μm (65 THz) instead of the entire spectrum were considered since the transmission behavior is not as affected by material variations at higher wavelengths.

The entire volumetric substrate of the FSS is discretized into 16 slabs resulting in a total of 3048 finite elements each with their own individual dielectric permittivity. The surface mesh details are given in Figure 8. Specifically, the substrates below FSS1 and above FSS2 are each discretized into 4 thickness layers with a surface mesh comprised of 162 ($9 \times 9 \times 2$)

and 200 ($10 \times 2 \times 2$) triangular surface elements, respectively. The substrate sandwiched between FSS1 and FSS2 is discretized into 8 layers, with each layer discretization into 200 ($10 \times 10 \times 2$) triangular surface elements.

For our design, the penalization factor was set to $n = 2$ and the volume fraction is set to $\eta = 60\%$. Validity of the simple mixture averaging formula was assured since the dimensions of the structure are much smaller as compared to the resonance wavelengths in the required pass-band region. Consequently, to achieve smooth mathematical convergence and to prevent intermediate material properties in the final design, a volume constraint was necessary. More specifically, sharper topologies with improved performance may be obtained if the volume constraint is active (satisfied as an equality) with the volume fraction yielding an approximate effective dielectric constant of around 3.3. This value corresponds to an average central resonance wavelength of the desired pass-band region. The solid material chosen for the design was Zinc Sulfide with $\varepsilon_{\text{solid}} = 4.84$. This would allow for 60% of solid material allocation via the active volume constraint and permit a feasible effective dielectric substrate to retain the required pass band behavior of 1-2.4 μm. This 60% of solid material was preferred in order to simplify the fabrication of the designed filter. With a volume fraction of ($\eta = 60\%$ and an initial air-like structure ($\varepsilon_{\text{initial}} = 1.1$), the resulting effective dielectric constant would be $4.84 * 0.6 + 1.1 * 0.4 \sim 3.3$.

The standard design algorithm was applied and convergence was achieved in 23 iterations as depicted in Figure 9. Remarkable improvement was achieved for the transmission response as compared to the initial performance (Figure 10). Key to achieving this performance was the optimal distribution of the available material within the 16 layers of the design domain (as illustrated by the density distribution in Figure 10). Figure 11 is actually a gray-scale cross section image of each layer with each grey-shade level corresponding to a specific range of ε_r values.
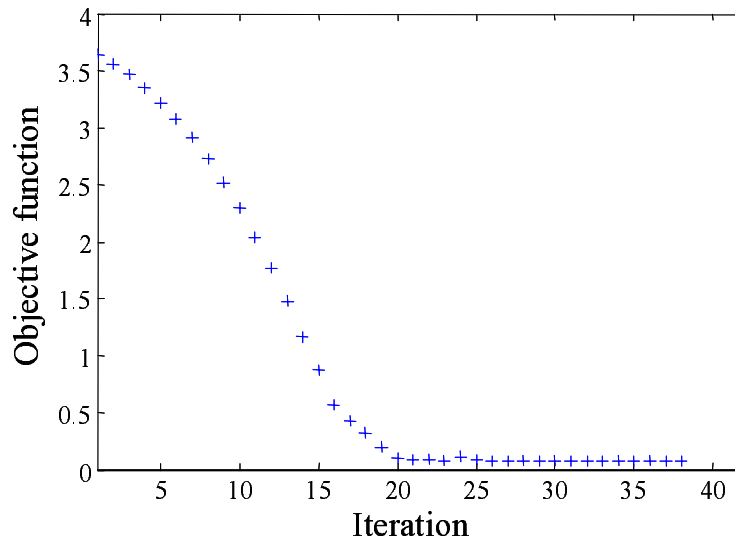

Figure 9. Optimization history for the spectral filter design with double layer FSS geometry (Figure 8). Design parameters: $n = 2$, $\eta = 60\%$, $\varepsilon_{\text{solid}} = 4.84$ (ZiS) and $\varepsilon_{\text{initial}} = 1.1$
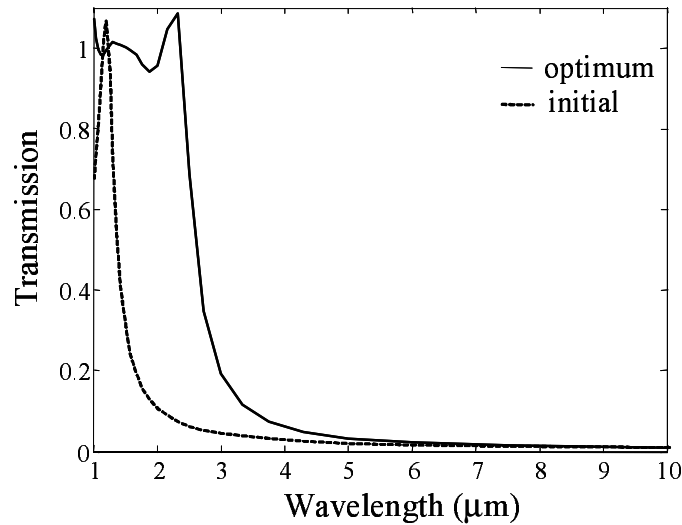
Figure 10. Transmission response for the initial ($\varepsilon = 1.1$) vs. the optimized material distribution of the TPV filter employing the double layer FSS geometry (Figure 8). Design parameters: $n = 2$, $\eta = 60\%$, $\varepsilon_{\text{solid}} = 4.84$ (ZnS) and $\varepsilon_{\text{initial}} = 1.1$

Manufacturing of the above material distribution presents us with several challenges. The distorted shapes at the outer edges of the solid (dark) material would present difficulties during the manufacturing stage. Also, the presence of a subtle amount of intermediate material within the light shade pixels (ε is not equal to 1.1 but larger than 1.34) presents a manufacturing challenge. The former is attributed to the meshing approach, which is restricted to triangular surface elements only. The latter is a typical issue encountered in topology optimization problems using SIMP. Several options are proposed to overcome these issues. Increasing the penalization factor is one such approach and more details relating to these approaches can be found in [13,25,26] but is not pursued here. The actual fabrication for the double layer FSS filter is a challenge to be explored. However, more recently success has been reported on manufacturing layers with the designed submicron dimensions [127].

5 CONCLUSIONS AND REMARKS

Two critical issues must be addressed in topology/material design. First, a general mathematical framework must be developed and adopted to conduct rigorous analysis of the composite materials without imposing any geometric and material restrictions. Second, a flexible design method is needed to find the best possible geometric configuration and material composition of the device. In this paper we adopted an extension of the Solid Isotropic Material with Penalization Method (SIMP) as the mathematical framework and integrated it with a fast hybrid finite-element boundary integral for EM analysis. The resulting design problem was solved using SLP. Like in any design approach, the goal in design is to allow for sufficient flexibility in geometry and materials choices so that novel devices can be generated. Summarizing, the design method must:

1. allow for shape and material design without a-priori information on the initial shape or topology,

2. incorporate versatile non-linear optimization methods based on well-defined optimization algorithms such as SLP,
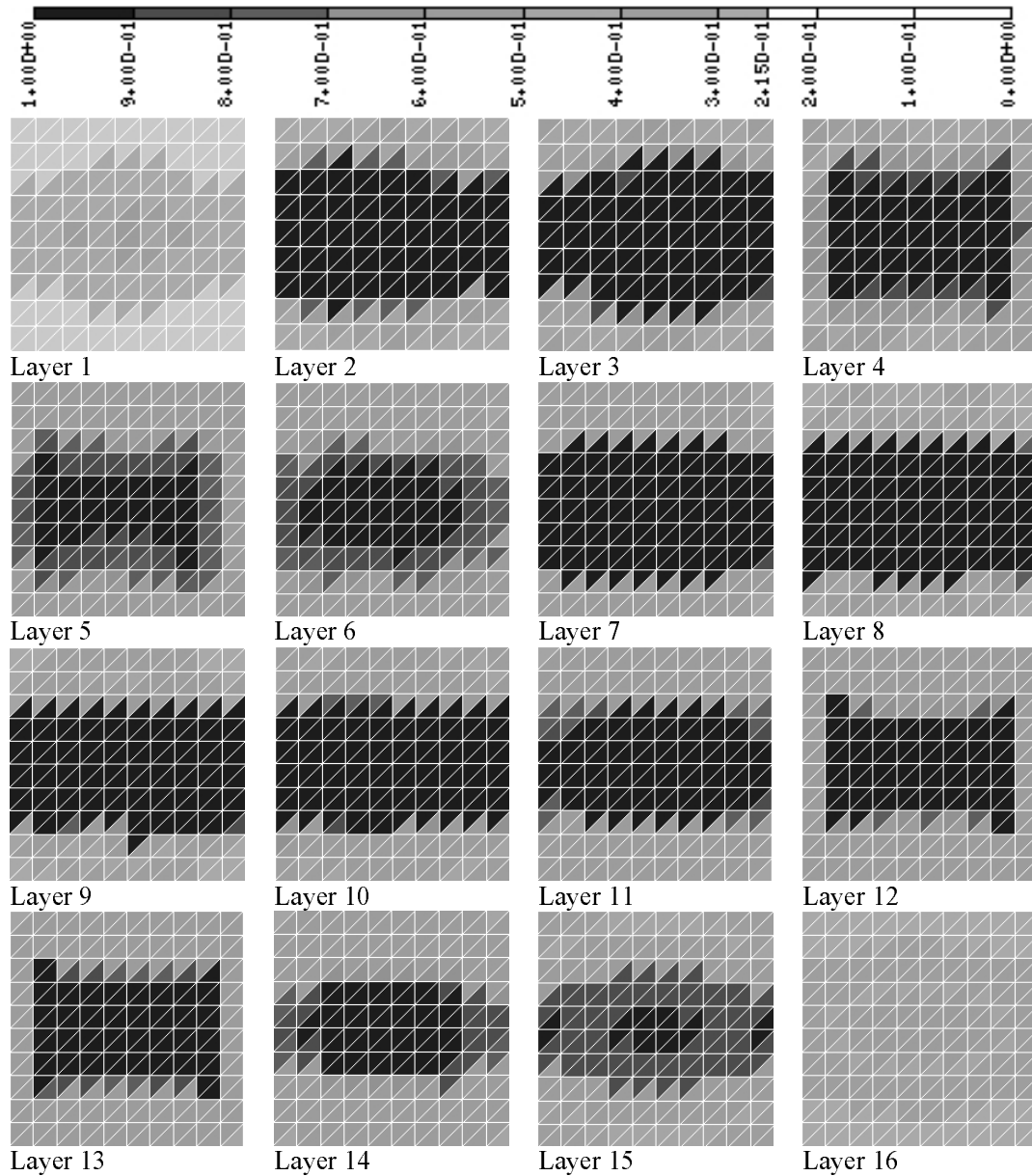
Figure 11. Optimized material distribution across each layer (counted from bottom) for TPV filter with double layer FSS geometry (Figure 8). Design parameters: $n = 2$, $\eta = 60\%$, $\varepsilon_{\mathrm{solid}} = 4.84$ (ZnS) and $\varepsilon_{\mathrm{initial}} = 1.1$

3. employ a simple continuous function to relate the actual material property to the introduced density variable (and is hence well-posed and computationally efficient),

4. update the design variables thru a sensitivity analysis via the adjoint variable method and permit full interface with the FE-BI electromagnetic solver.

To demonstrate the capability of the proposed design method, two design examples were used: a patch antenna and a spectral filter. For both design cases, significant performance

improvement was attained via optimization of the dielectric material topology. For manufacturing purposes, the resulting gray scale design for the antenna substrate was however altered via image processing/filtering to achieve a realizable/manufacturable solid design. Solidification of the dielectric substrate for the spectral filter design was still needed possibly through gradual penalization and continuation techniques. For applications based on more advanced materials, the SIMP model as well as the analysis module need be revised for improved accuracy and meshing capability.

Material compositions (topology) developed from 'scratch' (and possibility to include metallizations, 3D periodic or aperiodic, multilayers, etc.) is at the heart of design to realize not only bandpass filters or broadband antennas, but also materials which have other unique properties (including magnetic, impedance or specific value) and anisotropies that lead to designs never imagined or expected based on the existing portfolio of structures. The simplicity and low number of iterations needed to reach convergence motivate the application of the proposed method for other radiation and scattering applications.

REFERENCES

1 Kyriazidiou, C.A., Diaz, R.E. and Alexopoulos, N.G. (2000). Novel material with narrow-band transparency window in the bulk. *IEEE Trans. on Antennas and Propagation*, **48**, (**1**), 107–116.

2 Smith, D.R., Vier, D.C., Kroll N. and Schultz, S. (2000). Direct calculation of permeability and permittivity for a left-handed metamaterial. *Applied Physics Letters*, **77**, (**14**), 2246–2248.

3 Gauthier, G.P., Courtay, A. and Rebeiz, G.M. (1997). Microstrip antennas on synthesized low dielectric-constant substrates. *IEEE Trans. on Antennas and Propagation*, **45**, (**8**), 1310–1314.

4 Johnson, J.M. and Rahmat-Samii, Y. (1999). Genetic algorithms and method of moments (GA/MoM) for the design of integrated antennas. *IEEE Trans. on. Antennas and Propagation*, **47**, (**10**), 1606–1614.

5 Michielssen, E., Sajer, J.M., Ranjithan, S. and Mittra, R. (1993). Design of light-weight, broadband microwave absorbers using genetic algorithms. *IEEE Trans. on Microwaves Theory and Techniques*, **41**, (**6/7**), 1024–1031.

6 Li, Z., Erdemli, Y.E., Volakis, J.L. and Papalambros, P.Y. (2002). Design optimization of conformal antennas by integrating stochastic algorithms with the hybrid finite element method. *IEEE Trans. on AP*, **50**, (**5**), 676–684.

7 Li, Z., Volakis, J.L. and Papalambros, P.Y. (1997). Designing broad-band patch antennas using the sequential quadratic programming method. *IEEE Trans. on Antennas and Propagation*, **45**, (**11**), 1689–1692.

8 Dyck, D.N., Lowther, D.A. and Freeman, E.M. (1994). A method of computing the sensitivity in electromagnetic quantities to changes in materials and sources. *IEEE Trans. on Magnetics*, **30**, (**5**), 3415-3418.

9 Yoo, J., Kikuchi, N. and Volakis, J.L. (2000). Structural optimization in magnetic devices by the homogenization design method. *IEEE Trans. on Magnetics*, **36**, (**3**), 574–580.

10 Maxwell, J.C. (1873). *A Treatise on Electricity and Magnetism*, Oxford: Clarendon Press.

11 Lagrange, J.L. (1770). In *Royal Society of Turin*, 123.

12 Marrocco, A. and Pironneau, O. (1978). Optimum design with lagrangian finite elements: design of an electromagnet. *Comput. Methods Appl. Mech. Eng.*, **15**, 277–308.

13 Hadamard, J. (1932). *Le probleme de Cauchy et les equations aux derivees partielles lineaires hyperboliques.* Hermann, Paris.

14 Rao, S. (1996). *Engineering Optimization: Theory and Practice.* 3rd ed., Wiley, New York.

15 Nakata, T. and Takahashi, N. (1983). New design method of permanent magnets by using the finite element method. *IEEE Trans. on Magnetics*, **19**, 2494–249.

16 Hoole, S., Ratnajeevan, H., Subramaniam, S., Saldanha, R., Coulomb, J.L. and Sabonnadiere, J.C. (1991). Inverse problem methodology and finite elements in the identification of cracks, sources, materials, and their geometry in inaccessible locations. *IEEE Trans. on Magnetics*, **27**, 3433–3443.

17 Davis, L. (1987). *Genetic Algorithms and Simulated Annealing*, Pitman, London.

18 Holland, J. (1975). *Adaptation in Natural and Artificial Systems*. University of Michigan Press, Ann Arbor.

19 Haupt, R. (1995). An introduction of genetic algorithms for electromagnetics. *IEEE Antennas and Propagation Magazine*, **37**, (**2**), 7–15.

20 Johnson, J.M. and Rahmat-Samii, Y. (1997). Genetic algorithms in engineering electromagnetics. *IEEE Antennas and Propagation Magazine*, **39**, (**4**), 7–25.

21 Johnson, J.M. and Rahmat-Samii, Y. (1994). Genetic algorithm optimization and its application to antenna design. *IEEE Antennas and Propagation International Symposium*, Seattle, WA, USA.

22 Simkin, J. and Trowbridge, C.W. (1991). Optimizing electromagnetic devices combining direct search methods with simulated annealing. *Computation of Electromagnetic Fields (COMPUMAG)*, Sorrento, Italy.

23 Gottvald, A., Preis, K., Magele, C., Biro, O. and Savini, A. (1991). Global optimization methods for computational electromagnetics. *Computation of Electromagnetic Fields (COMPUMAG)*, Sorrento, Italy.

24 Xueying, J., Xueqin, S. and Qingxin, Y. (1993). The application of expert system to electromagnet design. *International Conference on Electromagnetic Field Problems and Applications*, Beijing, 1993.

25 Mohammed, O.A., Park, D.C., Uler, F.G. and Ziqiang, C. (1992). Design optimization of electromagnetic devices using artificial neural networks. *International Magnetics Conference (INTERMAG'92)*, St. Louis, MO, USA.

26 Enokizono, M. and Tsuchida, Y. (1994). Optimal design by boundary element method with fuzzy inference. *9th Conference on the Computation of Electromagnetic Fields (COMPUMAG'93)*, Miami, FL, USA.

27 Vivier, S., Gillon, F. and Brochet, P. (2001). Optimization techniques derived from experimental design method and their application to the design of a brushless direct current motor. *IEEE Trans. on Magnetics*, **37**, 3622–3626.

28 Gillon, F. and Brochet, P. (2000). Screening and Response Surface Method applied to the numerical optimization of electromagnetic devices. *12th Conference of the Computation of Electromagnetic Fields (COMPUMAG'99)*, Sapporo, Japan.

29 Preis, K., Magele, C. and Biro, O. (1990). FEM and evolution strategies in the optimal design of electromagnetic devices. *International Magnetics Conference INTERMAG*, Brighton, UK.

30 Bellina, F., Campostrini, P., Chitarin, G., Stella, A. and Trevisan, F. (1991). Automated optimal design techniques for inverse electromagnetic problems. *Computation of Electromagnetic Fields (COMPUMAG)*, Sorrento, Italy.

31 Sikora, J., Stodolski, M. and Wincenciak, S. (1988). Comparative analysis of numerical methods for shape designing. In *Electromagnetic Fields in Electrical Engineering*. A. Savini and J. Turowski (ed.), Plenum Press, New York, 293–298.

32 Li, Z., Papalambros, P.Y. and Volakis, J.L. (2002). Frequency selective surface design by integrating optimization algorithms with fast numerical methods. *IEE Proceedings-Microwaves, Antennas and Propagation*, **149**, (**3**), 175–180.

33 Pawluk, K. and Rudnicki, M. (1988). The state of art in the synthesis of electromagnetic fields. In *Electromagnetic Fields in Electrical Engineering*. A. Savini and J. Turowski (ed.), Plenum Press, New York, 287–292.

34 Guarnieri, M. Stella, A. and Trevisan, F. (1990). A methodological analysis of different formulations for solving inverse electromagnetic problems. *IEEE Trans. on Magnetics*, **26**, 622–625.

35 Takahashi, N. (1990). Optimal design method of magnetic circuit. *COMPEL - The International Journal for Computation and Mathematics in Electrical and Electronic Engineering*, **9**, 101–6.

36 Borghi, C.A., Di Barba, P., Fabbri, A., Rudnicki, M. and Savini, A. (2000). A benchmark problem in inverse magnetostatics solved by different multi-objective optimisation methods. *International Journal of Applied Electromagnetics and Mechanics*, **12**, 219–27.

37 Neittaanmaki, P., Rudnicki, M. and Savini, A. (1996). *Inverse Problems and Optimal Design in Electricity and Magnetism*. Vol. 1., Clarendon Press, Oxford, U.K.

38 Armstrong, A., Fan, M., Simkin, J. and Trowbridge, C.W. (1981). Automated optimization of magnet design using the boundary integral method. *Conference on the Computation of Electromagnetic Fields*, Chicago, IL, USA.

39 Di Barba, P., Navarra, P., Savini, A. and Sikora, R. (1990). Optimum design of iron-core electromagnets. *Conference of the Computation of Electromagnetic Fields*, Tokyo, Japan.

40 Di Barba, P. and Savini, A. (1999). Optimal shape design of an iron-cored electromagnet: A further benchmark problem in magnetostatics. *International Journal of Applied Electromagnetics and Mechanics*, **10**, 371–379.

41 Takahashi, N., Nakata, T. and Uchiyama, N. (1989). Optimal design method of 3-D nonlinear magnetic circuit by using magnetization integral equation method. *International Magnetics Conference*, Washington, DC, USA.

42 Gottvald, A. (1989). Optimal magnet design for NMR. *Conference on the Computation of Electromagnetic Fields (COMPUMAG)*, Tokyo, Japan.

43 Iwamura, Y. and Miya, K. (1989). Numerical approach to inverse problem of crack shape recognition based on the electrical potential method (of NDT). *Conference on the Computation of Electromagnetic Fields (COMPUMAG)*, Tokyo, Japan.

44 Hoole, S., Ratnajeevan, H. and Subramaniam, S. (1992). Inverse problems with boundary elements: Synthesizing a capacitor. *COMPUMAG Conference on the Computation of Electromagnetic Fields*, Naples, Italy.

45 Caminhas, W.M., Saldanha, R.R. and Mateus, G.R. (1990). Optimization methods used for determining the geometry of shielding electrodes. *IEEE Trans. on Magnetics*, **26**, 642–645.

46 Tsuboi, M. and Misaki, T. (1988). The optimum design of electrode and insulator contours by nonlinear programming using the surface charge simulation method. *IEEE Trans. on Magnetics*, **24**, 35–38.

47 Sikora, J., Skoczylas, J., Sroka, J. and Wincenciak, S. (1985). The use of the singular value decomposition method in the synthesis of the Neumann's boundary problem. *COMPEL - The International Journal for Computation and Mathematics in Electrical and Electronic Engineering*, **4**, 19–27.

48 Liu, J., Freeman, E.M., Yang, X. and Jianni, S. (1990). Optimization of electrode shape using the boundary element method. *IEEE Trans. on Magnetics*, **26**, 2184–2186.

49 Sikora, J. (1989). Minimax approach to the optimal shape designing of the electromagnetic devices. *COMPEL-The International Journal for Computation and Mathematics in Electrical and Electronic Engineering*, **8**, 162–175.

50 Franzone, P.C. (1980). Regularization methods applied to an inverse problem in electrocardiology. In *Computing methods in applied sciences and engineering*, R. Glowinski and J.L. Lions (eds.), North-Holland, New York, 615–633.

51 Duan, D.W. and Rahmat-Samii, Y. (1995). Generalized diffraction synthesis technique for high performance reflector antennas. *IEEE Trans. on Antennas and Propagation*, **43**, 27–40.

52 Haupt, R L. (1994). Thinned arrays using genetic algorithms. *IEEE Trans. on Antennas and Propagation*, **42**, 993–999.

53 Linden, D.S. and Altshuler, E.F. (1996). Automating wire antenna design using genetic algorithms. *Microwave Journal*, **39**, 7.

54 Davis, D., Chan, C. and Hwang, J. (1991). Frequency selective surface design using neural networks inversion based on parameterized representations. *Antennas and Propagation Society Symposium London, Ont., Can.*, **1**, 200–203.

55 Erdemli, Y., Sertel, K., Gilbert, R.A., Wright, D.E. and Volakis, J. (2002). Frequency selective surfaces to enhance performance of broadband reconfigurable arrays. *IEEE Trans. on Antennas and Propagation*, **50**, (**2**), 1716–1724.

56 Knott, E.F., Schaeffer, J.F. and Tuley, M.T. (1985). *Radar Cross Section- its Prediction Measurement and Reduction*. Artech House.

57 Ilavarasan, P., Rothwell, E.J., Chen, K. and Nyquist, D.P. (1995). Natural resonance extraction from multiple data sets using genetic algorithm. I*EEE Trans. on Antennas and Propagation*, **43**, 900–904,

58 Rekanos, I.T. (2002). Inverse scattering in the time domain: An iterative method using an FDTD sensitivity analysis scheme. *IEEE Trans. on Magnetics*, **38**, 1117–1120.

59 Kohn, R.V. and Strang, G. (1986). Optimal design and relaxation of variational problems. *Comm. Pure Appl. Math.*, **39**, 1–25 (Part I), 353–377 (Part II).

60 Galileo, G. (1638). *Discorsi e dimostrazioni matematiche*. Leiden.

61 Courant, R. (1943). Variational methods for the solution of problems of equilibrium and vibration. *Bull. Am. Math. Society*, **49**, 1–23.

62 Clough, R.W. (1960). The finite element in plane stress analysis. *Proc. 2nd ASCE Conference on Electronic Computation*, Pittsburgh, PA, USA.

63 Zienkiewicz, O.C. (1971). *The Finite Element Method in Engineering Science*. McGraw Hill, London.

64 Schmit, L.A. (1960). Structural design by systematic synthesis. *Proc. 2nd ASCE Conference on Electric Computations*, Pittsburgh, PA.

65 Zienkiewicz, O.C., Taylor, R.L. and Too, J.M. (1971). Reduced integration technique in general analysis of plates and shells. *Int. J. Numer. Methods Eng.*, **3**, 275–90.

66 Venkayya, V.B. (1978). Structural Optimization: A Review and Some Recommendations. *Int. J. Numer. Methods Eng.*, **13**, 203–228.

67 Olhoff, N. and Taylor, J.E. (1983). On Structural Optimization. *J. Appl. Mech. Trans. ASME*, **50**, 1139–1151.

68 Haslinger, J. and Neittaanmaki, P. (1988). *Finite Element Approximation for Optimal Shape Design: Theory and Applications*. Wiley, Chichester.

69 Weeber, K., Ratnajeevan, S. and H. Hoole. (1993). Structural design optimization as a technology source for developments in the electromagnetics domain. *5th Biennial IEEE Conference on Electromagnetic Field Computation*, Claremont, CA, USA.

70 Michell, A.G.M. (1904). The limits economy in frame structures. *Philo. Mag.*, **8**, 589–597.

71 Rozvany, G.I.N. (1972). Grillages of maximum strength and maximum stiffness. *Int. J. Mech. Sci.*, **14**, 651–666.

72 Rozvany, G.I.N., Zhou, M. and Birker, T. (1992). Generalized shape optimization without homogenization. *Structural Optimization*, **4**, 250–252.

73 Rozvany, G.I.N. (2001). Aims, scope, methods, history and unified terminology of computer-aided topology optimization in structural mechanics. *Structural and Multidisciplinary Optimization*, **21**, 90–108.

74 Bendsoe, M.P. and Kikuchi, N. (1988). Generating optimal topologies in structural design using a homogenization method. *Comp. Meth. Appl. Mech. Engng.*, **71**, 197–224.

75 Diaz, A. and Kikuchi, N. (1992). Solutions to shape and topology eigenvalue optimization problems using a homogenization method. *Int. J. Numer. Methods Eng.*, **35**, 1487–1502.

76 Bendsoe, M.P. (1989). *Methods for the Optimization of Structural Topology, Shape and Material.* Springer, New York.

77 Haber, R.B., Bendsoe, M.P. and Jog, C.S (1996). A new approach to variable topology shape design using a constraint on the perimeter. *Structural Optimization*, **11**, 1–12.

78 Allaire, G. and Kohn, R. (1993). Explicit bounds on the elastic energy of a two-phase composite in two space dimensions. *Q. Appl. Math.*, **51**, 675–699.

79 Bendsoe, M.P. (1989). Optimal shape design as a material distribution problem. *Structural Optimization*, **1**, 193–202.

80 Yang, R.J. and Chahande, A.I. (1995). Automotive applications of topology optimization. *Structural Optimization*, **9**, 245–249.

81 Bendsoe, M.P. (1995). *Optimization of Structural Topology, Shape and Material.* Springer, Berlin.

82 Sankaranarayanan, S., Haftka, R.T. and Kapania, R.K. (1993). Truss topology optimization with simultaneous analysis and design. *Structural Dyn. Mat. Conf.*, Dallas.

83 Bruns, T.E. and Tortorelli, D.A. (2001). Topology optimization of non-linear elastic structures and compliant mechanisms. *Computer Methods in Applied Mechanics and Engineering*, **190**, 3443–3459.

84 Ansanthasuresh, G.K. (1994). A new design paradigm for micro-electro mechanical systems and investigations on the compliant mechanism synthesis. In *Mechanical Engineering.* University of Michigan, Ann Arbor.

85 Hetrick, J.A., Kikuchi, N. and Kota, S. (1999). Robustness of compliant mechanism topology optimization formulations. *Smart Structures and Materials-Mathematics and Control in Smart Structures*, Newport Beach, CA, USA.

86 Ma, Z.D., Kikuchi, N. and Hagiwara, I. (1993). Structural topology and shape optimization for a frequency response problem. *Computational Mechanics*, **13**, 157–174.

87 Bloembaum, B. (1999). The use of structural optimization in automotive design-state of the art and vision. *WCSMO-3*, Buffalo.

88 Hassani, H. and Hinton, E. (1998). *Homogenization and Structural Topology Optimization Theory, Practice and Software.* Springer, Berlin.

89 Silva, E.C.N. , Fonseca, J.S.O. and Kikuchi, N. (1997). Optimal design of piezoelectric microstructures. *Comp. Mechanics*, **19**, 397–410.

90 Dyck, D.N. and Lowther, D.A. (1996). Automated design of magnetic devices by optimizing material distribution. *IEEE Transactions on Magnetics*, **32**, 1188–1193.

91 Gitosusastro, S., Coulomb, J.I. and Sabonnadiere, J.C. (1988). Performance derivative calculations and optimization process. *Third Biennial Conference on Electromagnetic Field Computation*, Washington, DC, USA.

92 Dyck, D.N., Lowther, D.A. and Freeman, E.M. (1994). A method of computing the sensitivity of electromagnetic quantities to changes in materials and sources. *IEEE Trans. on Magnetics*, **30**, 3415–3418.

93 Byun, J.K. and Hahn, S.Y. (1999). Topology optimization of electrical devices using mutual energy and sensitivity. *IEEE Trans. on Magnetics*, **35**, 3718–3720.

94 Wang, S. and Kang, J. (2002). Topology optimization of nonlinear magnetostatics. *IEEE Trans. on Magnetics*, **38**, 1029–1032.

95 Byun, J.K., Lee, J.H., Park, I.H., Lee, H.B., Choi, K. and Hahn, S.Y. (2000). Inverse problem application of topology optimization method with mutual energy concept and design sensitivity. *IEEE Trans. on Magnetics*, **36**, 1144–1147.

96 Koh, C.S. and Hahn, S.Y. (1993). A continuum approach in shape design sensitivity analysis of magnetostatic problems using the boundary element method. *IEEE Trans. on Magnetics*, **23**, 1771–1774.

97 Park, I.H., Lee, H.B., Kwak, I.G. and Hahn, S.Y. (1994). Design sensitivity analysis for steady state eddy current problems by continuum approach. *9th Conference on the Computation of Electromagnetic Fields (COMPUMAG'93)*, Miami, Fl, USA.

98 Dyck, D.N. (1995). Automating the topological design of magnetic devices. In *Electrical Engineering*, McGill University.

99 Lee, H.B. (1995). *Computer aided optimal design methods for waveguide structures*. Seoul National University.

100 Dyck, D.N. and Lowther, D.A. (1997). Composite microstructure of permeable material for the optimized material distribution method of automated design. *IEEE Trans. on Magnetics*, **33**, 1828–1831.

101 Choi, S.H.E., Lowther, D.A. and Dyck, D.N. (1997). Determining boundary shapes from the optimized material distribution system. *11th International Conference on Computation of Electromagnetic Fields (COMPUMAG)*, Rio de Janeiro, Brazil.

102 Dyck, D.N. and Lowther, D.A. (1998). Response surface modelling of magnetic device performance using function value and gradient. *International Journal of Applied Electromagnetics and Mechanics*, **9**, 241–248.

103 Chung, Y.S., Cheon, C. and Hahn, S.Y. (2000). Reconstruction of dielectric cylinders using FDTD and topology optimization technique. *IEEE Trans. on Magnetics*, **34**, 956–959.

104 Chung, Y.S. and Cheon, C. (2001). Optimal shape design of dielectric structure using FDTD and topology optimization. *International Microwave Symposium*, Phoenix, AZ, USA.

105 Wang, S. and Kim, C. (2000). A study on the topology optimization of electromagnetic systems. *CEFC 2000.*

106 Bossavit, A. (1994). Effective penetration depth in spatially periodic grids: a novel approach to homogenization. *International Symposium on Electromagnetic Compatibility*, Rome, Italy.

107 Gong, J., Volakis, J.L., Woo, A.C. and Wang, H.T.G. (1994). Hybrid finite element-boundary integral method for the analysis of cavity-backed antennas of arbitrary shape. *IEEE Trans. on Antennas and Propagation*, **42**, 1233–1242.

108 Jin, J.M. and Volakis, J.L. (1991). A finite-element-boundary integral formulation for scattering by three-dimensional cavity-backed apertures. *IEEE Trans. on Antennas and Propagation*, **39**, (**1**), 97–104.

109 Lucas, E.W. and Fontana, T.P. (1995). 3-D hybrid finite element/boundary element method for the unified radiation and scattering analysis of general infinite periodic arrays. *IEEE Trans. on Antennas and Propagation*, **43**, 145–153.

110 Volakis, J., Chatterjee, A. and Kempel, L. (1998). Finite Element Method for Electromagnetics: Antennas, Microwave Circuits and Scattering Applications. *IEEE Press*, New York.

111 Sigmund, O. and Petersson, J. (1998). Numerical instabilities in topology optimization: a survey on procedures dealing with checkerboards, mesh-dependencies and local minima. *Structural Optimization*, **16**, 68–75.

112 Hanson, R. and Hiebert, K. (1981). *A sparse linear programming subprogram.* Sandia National Laboratories SAND81-0297.

113 Schittkowski, K., Zillober, C. and Zotemantel, R. (1994). Numerical comparison of nonlinear programming algorithms for structural optimization. *Structural Optimization*, **7**, 1–19.

114 Thomas, H.L., Vanderplaats, G.N. and Shyy, Y.K. (1992). A study of move-limit adjustment strategies in the approximation concepts approach to structural analysis. *4th AIAA/USAF/NASA/OAI Symposium on Multidisciplinary Analysis and Optimization*, Cleveland, Ohio.

115 Director, S.W. and Rohrer, R.A. (1972). Introduction to Systems Theory. *McGraw-Hill Series in Electronics Systems.* McGraw-Hill Book Co, New York.

116 Kiziltas, G. (2003). Dielectric material optimization of filters and antennas using SIMP. In *Mechanical Engineering*, The University of Michigan, Ann Arbor.

117 Zurcher, J.F. and Gardiol, F.E. (1995). *Broadband Patch Antennas.* Artech House, Inc., Norwood, MA.

118 Hansen, R.C. (1981). Fundamental limitations on antennas. *Proceedings of IEEE*, **69**, 170–182.

119 Lee, H.F. and Chen, W. (1997). *Advances in Microstrip and Printed Antennas.* Wiley, New York.

120 Lech, M., Mitchell, A. and Waterhouse, R. (2000). Optimization of broadband microstrip patch antennas. *Asia-Pacific Microwave Conference*, Sydney, NSW, Australia.

121 Koh, B.Y., Halloran, J.W., Knapp, A.M., Volakis, J., Kiziltas, G. and Psychoudakis, D. (2003). Textured dielectric meta-materials for miniaturized antennas: fabrication of dielectric LTCC-polymer by thermoplastic green machining. *105th Annual Meeting & Exposition of The American Ceramic Society*, Nashville, TN.

122 Weile, D. and Michielssen, E. (1999). Design of doubly periodic filter and polarizer structures using a hybridized genetic algorithm. *Radio Science*, **34**, 51–63.

123 Wu, T.K. (1995). *Frequency Selective Surface and Grid Array.* Wiley, New York.

124 Weile, D.S. and Michielssen, E. (1997). Evolutionary optimization of electromagnetic devices using advanced operators and population structures. *Antennas and Propagation Society International Symposium*, Montreal, Que., Canada.

125 Wu, T.K. and Lee, S.W. (1994). Multiband frequency selective surface with multiring patch elements. *IEEE Trans. on Antennas and Propagation*, **42**, 1484–1490.

126 Munk, B.A. (2000). *Frequency Selective Surfaces: Theory and Design.* Wiley, New York.

127 Spector, S.J., Astolfi, D.K., Doran, S.P., Lyszczarz, T.M. and Raynolds, J.E. (2001). Infrared Frequency Selective Surfaces Fabricated Using Optical Lithography and Phase Shift Masks. *J. Vac. Sci. Technol. B.*, **19**, (**6**), 2757–2760.